UNIVERSITY OF CALIFORNIA

Ernest O. Lawrence Radiation Laboratory

BERKELEY, CALIFORNIA

DISCLAIMER

UCRL-1910
Unclassified-Physics Distribution

UNIVERSITY OF CALIFORNIA

Radiation Laboratory

Contract No. W-7405-eng-48

EFFECT OF CHEMICAL STRUCTURE ON STOPPING POWERS FOR HIGH-ENERGY PROTONS

Theos Jardin Thompson

(Thesis)

August 11, 1952

Berkeley, California

TABLE OF CONTENTS

TABLE OF CONTENTS

EFFECT OF CHEMICAL STRUCTURE ON STOPPING POWERS FOR HIGH-ENERGY PROTONS

Theos Jardin Thompson

Radiation Laboratory, Department of Physics
University of California, Berkeley, California

August 11, 1952

ABSTRACT

A study has been made of the stopping power of various elements and compounds for a high energy proton beam. The purpose of the measurements was twofold. First, an effort has been made to determine whether or not the relative stopping power of a compound is strictly an additive function of the elements which form the compound. Second, the stopping powers of four elements hydrogen, carbon, nitrogen, and oxygen and twenty-nine compounds of these elements have been measured with a high degree of accuracy. The stopping power of a fifth element, chlorine, has been inferred from its compounds.

All stopping powers were measured relative to copper. The definition used in this paper for the relative stopping power is:

$$S_{\text{compound}} = \frac{\left(\frac{\text{Range}}{\text{Mole wt.}}\right)_{\text{copper}}}{\left(\frac{\text{Range}}{\text{Mole wt.}}\right)_{\text{compound}}}$$

This is a relative molal stopping power. Proofs of the validity of this form as applied to additivity calculations are included in the paper.

The experimental method employed the use of the so-called "Bragg curve" method of determination of range. Almost all targets were chosen to reduce the mean beam energy from 340 Mev to 200 Mev. Others were corrected to this energy interval.

The results indicate that the stopping power of a compound as a whole is an additive function of the elements in the compound to within about 1 percent. The largest percentage deviations occur with the hydrogen and are of the order of 2 percent. The percentage deviations decrease rapidly with increasing atomic number. Thus the stopping power of chlorine in all compounds was essentially constant.

By using Bethe's Equation (XI) for ionization energy loss in an absorber, and assuming with Bakker and Segrè[9] that the mean ionization potential for copper as defined by Bethe's equation is given as 279 ev., the mean ionization potentials for the various elements in various compounds has been calculated. The resulting information is given below in tabular form.

Table I

Elements

Element	S	I
Hydrogen (Molecular)	0.0472 ± 0.0002 (est.)	18.2 ev.
Carbon (Graphite)	0.2455 ± 0.0005 (est.)	70.2 ev.
Nitrogen (Molecular)	0.2837 ± 0.0001 (est.)	76.3 ev.
Oxygen (Molecular)	0.3188 ± 0.0003 (est.)	88.3 ev.

Table II

Compounds

Element in Compound	Position in Compound	S	I
Hydrogen	Saturated	0.04797 ± 0.00007	15.5 ev.
	Unsaturated	0.04879 ± 0.00010	13.0
Carbon	Saturated	0.24627 ± 0.00016	69.3
	Unsaturated	0.24674 ± 0.00009	67.2
	Highly chlorinated	0.2509 ± 0.0008	57.9
Nitrogen	Amines, nitrates, etc.	0.2785 ± 0.0025	89.4
	In ring	0.2870 ± 0.0020	68.8
Oxygen	-O-	0.3187 ± 0.0024	88.5
	o=	0.3226 ± 0.0010	79.8
Chlorine	All	0.6335 ± 0.0035	153.7

If S_{cpd} and the range or (dE/dx), for copper is known, the defining equation above may be used to give in a simple way the range or (dE/dx) for the compound. The S_{cpd} for a compound A_aB_b may be calculated using the value tabulated above by use of the equation $S_{cpd} = aS_A + bS_B$.

EFFECT OF CHEMICAL STRUCTURE ON STOPPING POWERS FOR HIGH-ENERGY PROTONS

Theos Jardin Thompson

Radiation Laboratory, Department of Physics
University of California, Berkeley, California

August 11, 1952

II. INTRODUCTION

A. Background

The loss of energy in matter by fast moving charged particles has been an object of study for many years. It was early realized that this was due primarily to the excitation and ionization of the atoms traversed. Bohr[1], Bethe[2,3,4] and others have succeeded in explaining the phenomenon in some detail. Bohr made the first classical analysis. Bethe used the Born approximation applied to the collisions between heavy particles and the atomic electrons to develop his analysis. This development made use of quantum mechanics. The discussion here will be confined to a brief outline of the Bethe theory.

Bethe[2] considered the hydrogen atom and first calculated the differential cross section as a function of momentum for inelastic collisions. This corresponds to a transfer of energy to the atomic electrons and excites the struck electron to some given level, n, l, or to the continuum. The differential cross section for excitation to any given level, $d\Phi_n(q)$, as a function of momentum (q) is then integrated

over all possible momenta to give the total cross section for excitation to any given level, n. The momentum, q, is that exchanged in the collision and the cross section has the dimensions of an area. If this cross section then be multiplied by the energy difference between the ground state and the excited state, summed over all levels, n, and multiplied by N, the atomic density, the energy loss per centimeter by an incident particle is obtained.

$$-\frac{dE}{dx} = N \sum_n (E_n - E_o) \int_{q_{min}}^{q_{max}} d \Phi_n (q) \qquad (I)$$

This equation may be rewritten in terms of the probability matrix elements involved. The expression obtained by that operation may then be rewritten in terms of oscillator strengths (f_{nl}) for all possible transitions. By rearrangement, the latter expression may be simplified in terms of a mean excitation energy for all possible excitations of an electron originally in an atomic state n,l. The mean excitation energy of the n,l'shell ($A_{n,l}$) is defined by:

$$f_{nl} \log A_{nl} = f_{nl} \log (-E_{nl}) + \sum_{n'l'} f'_{nl,\, n'l'} \left(Z_{nl} - \frac{\overleftarrow{Z_{nl}} \overleftarrow{Z_{n'l'}} + \overrightarrow{Z_{nl}} \overrightarrow{Z_{n'l'}}}{g_{n'l'}} \right) \log \left(\frac{E_{n'l'} - E_{nl}}{-E_{nl}} \right) \qquad (II)$$

where E_{nl} is the ionization potential of the n,l shell, Z_{nl} is the number of electrons in the n,l shell in the ground state, $\overleftarrow{Z_{nl}}$ and $\overrightarrow{Z_{nl}}$ are the

number of n,l electrons of shell n,l in a single spin direction. $Z_{nl} = (\overleftarrow{Z_{nl}} + \overrightarrow{Z_{nl}})$ and $g_{nl} = 2\,l + 1$ is the weight of the electronic state (n, l). In terms of this mean excitation energy for all possible states excited from an original state n,l, the energy loss per centimeter may be written:

$$-\frac{dE}{dx} = \frac{4\pi e^4 z^2}{mv^2} N\Sigma f_{nl} \log \frac{2mv^2}{A_{nl}} \qquad \text{(III)}$$

A mean excitation potential I for the atom as a whole may now be defined by the equation:

$$Z \log I = \sum_{nl} f_{nl} \log A_{nl} \qquad \text{(IV)}$$

In terms of this equation we may write the energy loss per centimeter:

$$-\frac{dE}{dx} = \frac{4\pi e^4 z^2 Z}{mv^2} N \log \frac{2mv^2}{I} \qquad \text{(V)}$$

Calculations using this equation modified as indicated below to account for relativistic effects give values for I which are much too low. In a more recent article[3] and in private conversations, Bethe suggests following the procedure first advanced by Blackett[5] and used later by Duncanson[6], etc. This involves using the equation in the form given below together with experimentally measured values of dE/dx to calculate values for I.

For atomic hydrogen the equation given by Bethe is as follows:

$$-\frac{dE}{dx} = \frac{4\pi e^4 N}{mv^2} \log \frac{mv^2}{1.105\ \text{Ry}\ h} \qquad \text{(VI)}$$

Ry in this case is the Rydberg constant. Thus the value of I for hydrogen should be somewhat higher than that of the ordinary ionization potential for the hydrogen atom.

In a more generalized form, Bethe[2] has shown that the energy loss for nuclear particles per centimeter of target material thickness can be given by:

$$-\frac{dE}{dx}(\text{cm.}) = \frac{4\pi e^4 z^2 N}{mv^2}\left\{Z\left(\log\frac{2mv^2}{I(1-\beta^2)}-\beta^2\right)-\frac{C_k}{Z}\right\} \qquad \text{(VII)}$$

Here dE/dx is given for particles of charge ez and speed v moving through an absorber of effective nuclear charge Z, effective ionization potential per atom I, and with atomic density N. Note that $\beta = v/c$ where c is the velocity of light. C_k is a correction term representing the deficiency of stopping power of the K shell electrons at relatively lower incident particle energies but unimportant for the high speed incidence protons employed in this experiment. Bethe has also developed the concept of stopping number. This is a convenient dimensionless quantity (B) proportional to the stopping power.

$$B = Z \log 2\frac{mv^2}{I} \qquad \text{(VIII)}$$

As stated above, I is usually treated as an empirical constant to be fixed by the substitution of known data in Equation (I). Through the years many workers[7,8,9,10] have measured experimental values for (dE/dx) and range and from these experiments values have been calculated

for I for many elements. As an approximation, Bloch[12] has shown that I may be given as:

$$I = aZ \qquad \text{(IX)}$$

where a is a constant of proportionality varying slightly from element to element, and Z is the atomic number of the stopping medium. It has been shown experimentally that a varies from approximately 16 electron volts for hydrogen to approximately 9.5 electron volts for the heavier elements[7,9,10,11,12,13,14].

The Bethe equation (VII) above holds accurately only at particle velocities well above those of the oribital electrons in the target atoms. Thus to obtain the closest agreement with Bethe's theory, experiments should be conducted using high velocity heavy incident particles.

B. Statement of Problem

It is a matter of some theoretical interest to know whether or not, and by how much, the mean ionization potential, I, of an element will be altered if the element considered is a part of a compound. It is also a matter of interest to experimental nuclear physicists interested in accurate measurements of stopping power and ionization losses in targets and absorbers to know how much the effect of I alteration in compounds may be. The effect on I if the element used is in a compound is expected to be small since in formation of molecules only the outermost, or valence, electron shell is involved. Even in the outer shell the changes will not be too great. Thus the percentage change in effective I for high atomic

number elements cannot be expected to be large. One would expect the percentage change in I and hence (dE/dx) values to be greater in the lower elements and thus probably greatest in hydrogen. As it is to be expected that the effects will be small, the measurements must be made accurately. Thus, as an incidental part of the experiment the stopping power and hence, indirectly, I for certain pure elements may be obtained with a high precision.

Specifically, the principal purpose of this experiment has been to determine whether or not the relative stopping power of various compounds for a high energy proton beam is strictly an additive function of the elements which make up the compound.

C. Basis of Calculation Method

In order to calculate the relative stopping power of the various compounds and elements, copper was chosen as the basic material.

The definition used in this experiment for the relative stopping power to copper is:

$$S_{cpd} = \frac{\left[\frac{R\left(\frac{gms}{cm^2}\right)}{M}\right]_{cu}}{\left[\frac{R\left(\frac{gms}{cm^2}\right)}{M}\right]_{cpd}} = \left(\frac{R\,\frac{gms}{cm^2}}{M}\right)_{cu} x \left(\frac{M}{R\,\frac{gms}{cm^2}}\right)_{cpd} \qquad (X)$$

R is the proton range as measured experimentally. M is the molecular weight of the element or compound in question. This is a relative molal stopping power. The (R/M) for copper appears on the numerator. By writing it in this way a compound or element with a small R/M will give

a large "stopping power" or S value, that is, the compound or element is more effective per mole in stopping the proton beam than one with a larger R/M value.

This particular definition of the relative stopping power was chosen because of its straight forward application to calculation of the additivity effects of stopping power. To show this, assume that in the sample and in the comparison, we have a relatively small increment of energy lost and thus a small increment of the proton range, dR, is spent in the sample.

If L is the number of molecules per mole, ρ the density, and M the molecular weight, then $N = L\rho/M$ and Equation (VII) in terms of energy loss per gram-cm^{-2} may be rewritten for high energy incident protons:

$$-\frac{dE}{dx\left(\frac{gms}{cm^2}\right)} = \frac{4\pi z^2 e^4}{mv^2}\,\frac{L}{M}\left\{Z\left(\ln\frac{2mv^2}{I(1-\beta^2)} - \beta^2\right)\right\} \qquad (XI)$$

The increment of range may be written:

$$dR = \frac{dE}{f(E)} = \frac{dE}{\left(\frac{dE}{dX}\right)} \qquad (XII)$$

From $$S_{cpd} = \left(\frac{dR}{M}\right)_{cu}\left(\frac{M}{dR}\right)_{cpd} \qquad (XIII)$$

Now define $$M = aA + bB, \qquad (XIV)$$

where A = atomic weight of element A

B = atomic weight of element B

a = atoms of A per molecule

b = atoms of B per molecule

M = Molecular weight of the compound

Let us assume complete additivity and that the mean energy of the proton beam is the same at all points in any single plane passed through the sample perpendicular to the beam. Then the proton energy loss in passing between any two such planes will be the same as that in a mixture of the two elements in proper proportions and will be proportional to the fraction by weight of each element present multiplied by its energy loss per gram-cm^{-2}, i.e.,

$$\left(\frac{dE}{dx}\right)_{compound} = \left(\frac{dE}{dx}\right)_A \frac{aA}{M} + \left(\frac{dE}{dx}\right)_B \frac{bB}{M} \qquad \text{(XV)}$$

Substitution of (XI), (XII), and (XV) into (XIII) gives

$$S_{compound} = \frac{\left(\frac{dE}{\left(\frac{dE}{dx}\right)}\right)}{M_{cu}}_{cu} \left(\frac{M_{cpd}}{\frac{dE}{\left(\frac{dE}{dx}\right)_A \frac{aA}{M_{cpd}} + \left(\frac{dE}{dx}\right)_B \frac{bB}{M_{cpd}}}} \right) \qquad \text{(XVI)}$$

If the energy increment and the velocity considered is the same throughout, S_{cpd} may be rewritten:

$$S_{cpd} = \left(\frac{1}{\frac{4\pi z^2 e^4 Z_{cu}}{mv^2}\left(\ln \frac{2mv^2}{I_{cu}(1-\beta^2)} - \beta^2\right)} \right) \quad x \qquad \text{(XVII)}$$

$$\left(\frac{\frac{4\pi z^2 e^4}{mv^2}\left\{ aZ_A \left(\ln \frac{2mv^2}{I_A(1-\beta^2)} - \beta^2\right) + bZ_B \left(\ln \frac{2mv^2}{I_B(1-\beta^2)} - \beta^2\right)\right\}}{1} \right)$$

$$= \frac{aZ_A \left(\ln \frac{2mv^2}{I_A(1-\beta^2)} - \beta^2\right)}{Z_{cu}\left(\ln \frac{2mv^2}{I_{cu}(1-\beta^2)} - \beta^2\right)} + \frac{bZ_B \left(\ln \frac{2mv^2}{I_B(1-\beta^2)} - \beta^2\right)}{Z_{cu}\left(\ln \frac{2mv^2}{I_{cu}(1-\beta^2)} - \beta^2\right)}$$

or if the energy interval and the factors common to both numerator and denominator be replaced, it will be seen that:

$$S_{compound} = aS_A + bS_B \qquad \text{(XVIII)}$$

Thus, for small increments of energy dE the above relationship holds. Since the energy occurs only within the logarithm and as a small relativistic correction, the definition of stopping power given above will be almost independent of the incident energy so long as Bethe's Equation VII and XI hold. This is further justified as the ratio of the two logarithm factors will be even more closely a constant independent of the incident particle energy. It must now be considered whether or not the relationship of Equation XVIII is justified when integrated over larger energy intervals. Two methods of proof have been used. First, the expressions below were numerically integrated over a range from 340 to 200 Mev

for CH_2 and CH using the (dE/dx) values given in Aron's Tables[15] and the results compared. This integration represents the questionable step in the procedure. The (R/M) for copper will be the same on both sides of Equation XVIII.

$$\frac{M_{cpd}}{R_{cpd}} = \frac{M_{cpd}}{\int_{200}^{340} \frac{dE}{\left(\frac{dE}{dx}\right)_A \frac{aA}{M_{cpd}} + \left(\frac{dE}{dx}\right)_B \frac{bB}{M_{cpd}}}} \quad (?) \qquad \text{(XIXA)}$$

$$a\frac{M_A}{R_A} + \frac{bM_B}{R_B} = \frac{aM_A}{\int_{200}^{340} \frac{dE}{\left(\frac{dE}{dx}\right)_A}} + \frac{bM_B}{\int_{200}^{340} \frac{dE}{\left(\frac{dE}{dx}\right)_B}} \qquad \text{(XIXB)}$$

The results obtained are:

	XIXA	XIXB	Relative difference
CH	0.32319010	0.32318579	4.3×10^{-6}
CH_2	0.37538369	0.37538296	0.73×10^{-6}

A more convincing proof, perhaps, is that given below which was developed by Bethe in conversations with the author.

Equation XI may be written:

$$-\frac{dE}{dx\left(\frac{gms}{cm^2}\right)} = \frac{4\pi z^2 e^4}{mv^2} \frac{LZ}{M} \left[\ln \frac{2mv^2}{I} - \ln (1-\beta^2) - \beta^2\right]$$

Expanding $\ln(1-\beta^2)$

$$-\frac{dE}{dx} = \frac{4\pi z^2 e^4}{mv^2}\,\frac{LZ}{M}\left[\ln\frac{2mv^2}{I} + \frac{1}{2}\beta^4 + \frac{1}{3}\beta^6 \ldots\ldots\right]$$

At E = 340 Mev and I = 53.1 ev. $\ln 2mv^2/I = 9.09$ and $\beta^2 = 0.46$.

To order of β^4 one may neglect the relativistic corrections. The β^4 term above is 1.2 percent of the $\ln 2mv^2/I$ and will not appreciably affect the correction term to be worked out below.

Now define a new variable $X = 2mv^2$ then $dx = 4mvdv$ and $dE = mvdv = dx/4$, then:

$$R_A = \int_0^{E_{max}} \frac{dE}{\left(\frac{dE}{dx}\right)_A} = \int_0^{E_{max}} \frac{A\,2mv^2 dE}{8\pi z^2 e^4 LZ \ln\frac{2mv^2}{I_A}} = \frac{A}{KZ_A}\int_0^{X_{max}} \frac{XdX}{\ln\frac{X}{I_A}} \qquad (XX)$$

where $K = 32\pi z^2 e^4 L$ from Equations XI, XVI and XVII:

$$\frac{S_{cpd}}{M_{cpd}\left(\frac{R}{M}\right)_{cu}} = \frac{1}{R_{cpd}} = \frac{K}{\int_0^{X_{max}} \frac{XdX}{aZ_A \ln\frac{X}{I_A} + bZ_B \ln\frac{X}{I_B}}} \overset{(?)}{\simeq} \frac{aZ_A}{\int_0^{X_{max}} \frac{XdX}{\ln\frac{X}{I_A}}} + \frac{bZ_B}{\int_0^{X_{max}} \frac{XdX}{\ln\frac{X}{I_B}}} \qquad (XXI)$$

Now define an effective ionization potential for the compound by the following equation:

$$\ln I_{eff} = \frac{aZ_A \ln I_A + bZ_B \ln I_B}{aZ_A + bZ_B} \qquad (XXII)$$

Then Equation XXI may be written:

$$\frac{1}{R_{cpd}} = \frac{K}{\int_0^{X_{max}} \frac{XdX}{(aZ_A+bZ_B)\ln\frac{X}{I_{eff}}}} \overset{(?)}{\simeq} \frac{KaZ_A}{\int_0^{X_{max}} \frac{XdX}{\ln\frac{X}{I_A}}} + \frac{KbZ_B}{\int_0^{X_{max}} \frac{XdX}{\ln\frac{X}{I_B}}} \quad \text{(XXIII)}$$

Define a function F(I) by:

$$F(I) = \frac{1}{\int_0^{X_{max}} \frac{XdX}{\ln\frac{X}{I}}} \quad \text{(XXIV)}$$

In terms of F(I) Equation XXIII may be written:

$$\frac{1}{K}\left(\frac{S_{cpd}}{M}\right)_{cpd}\left(\frac{M}{R}\right)_{cu} = (aZ_A + bZ_B)\, F(I_{eff}) \overset{(?)}{=} aZ_A\, F(I_A) + bZ_B\, F(I_B) \quad \text{(XXV)}$$

Now expand $F(I_{eff})$ in a Taylor's expansion:

$$F(I_{eff}) = F\left(\ln I_o + \ln\frac{I_{eff}}{I_o}\right) = F(I_o) + F'(I_o)\left(\ln\frac{I_{eff}}{I_o}\right) + 1/2\, F''(I_o)\left(\ln\frac{I_{eff}}{I_o}\right)^2 + \ldots$$

and similarly for $F(I_A)$ and $F(I_B)$ (XXVI)

$$F(I_A) = F(I_o) + F'(I_o)\left(\ln\frac{I_A}{I_o}\right) + F''(I_o)\left(\ln\frac{I_A}{I_o}\right)^2 + \ldots. \text{ etc.}$$

$$\frac{1}{K}\left(\frac{S}{R}\right)_{cpd}\left(\frac{M}{R}\right)_{cu} = (aZ_A+bZ_B)\left[F(I_o) + F'(I_o)\left(\ln\frac{I_{eff}}{I_o}\right) + 1/2\, F''(I_o)\left(\ln\frac{I_{eff}}{I_o}\right)^2 + \ldots.\right]$$

$$\overset{(?)}{=} aZ_A\left[F(I_o) + F'(I_o)\ln\frac{I_A}{I_o} + 1/2\, F''(I_o)\left(\ln\frac{I_A}{I_o}\right)^2 + \ldots\right] + \quad \text{(XXVII)}$$

$$bZ_B\left[F(I_o) + F'(I_o)\ln\frac{I_B}{I_o} + \ldots..\right]$$

Substitution of the definition of I_{eff} given by Equation XXII in the first derivative expansion term of the left hand member above shows at once that the two sides of the equation are in agreement through the first derivative terms of the expansion. The difference between the two sides is then given by:

$$\Delta = 1/2\ F''(I_o)\left[aZ_A\left\{(\ln\frac{I_{eff}}{I_o})^2 - (\ln\frac{I_A}{I_o})^2\right\}+bZ_B\left\{(\ln\frac{I_{eff}}{I_o})^2-(\ln\frac{I_B}{I_o})^2\right\}\right] \quad \text{(XXVIII)}$$

+ higher order terms.

Now consider the function $F(I_o)$:

Let $\frac{X}{I_o} = e^{u/2}$ or $2\ln\frac{X}{I} = u$ then $dx = \frac{I_o}{2}\, e^{u/2}\, du$

$$\frac{1}{F(I_o)} = \int_0^{X_{max}} \frac{XdX}{\ln\frac{X}{I_o}} = \int_0^{u_{max}} \frac{I_o{}^2 e^u du}{u}$$

This is an exponential integral and its solution for $|u|>>1$ is given in Jahnke-Emde[16] is:

$$\overline{E_1(u)} = \frac{e^u}{u}\ H(u)$$

In our case u is approximately 18.)

where $$H(u) = 1 + \frac{1}{u}\,1 + \frac{2}{u^2}\,1 + \ldots\ldots$$

Note that this is a semiconvergent series.

$$F(I_o) = \left(\frac{1}{I_o{}^2}\right)\left(\frac{I_o{}^2}{X^2}\right) u\left(\frac{1}{1 + \frac{1}{u}1 + \frac{2}{u^2}1 + \ldots}\right) = \frac{u}{X^2}\left(\frac{1}{u} - \frac{1}{u^2} - \frac{3}{u^3} - \frac{13}{u^4} - \ldots\right)$$

$$= \frac{1}{X^2}\left(u - 1 - \frac{1}{u} - \frac{3}{u^2} \ldots\ldots\right)$$

$$F'(I_o) = \frac{1}{X^2}\left(1 + \frac{1}{u^2} + \frac{6}{u^3} + \ldots\ldots\right)$$

$$F''(I_o) = \frac{1}{X^2}\left(-\frac{2}{u^3} - \frac{24}{u^4} \ldots\ldots\right)$$

Using the first term of the expansion of $F''(I_o)$ and substituting in Equation XXVIII one obtains:

$$\Delta = -\frac{1}{X^2u^3}\left[aZ_A\left\{\left(\ln\frac{I_{eff}}{I_o}\right)^2 - \left(\ln\frac{I_A}{I_o}\right)^2\right\} + bZ_B\left\{\left(\ln\frac{I_{eff}}{I_o}\right)^2 - \left(\ln\frac{I_B}{I_o}\right)^2\right\}\right] \quad \text{(XXIX)}$$

$$+ \text{higher order terms}$$

From Equation XXV:

$$\frac{1}{K}\left(\frac{S}{M}\right)_{cpd}\left(\frac{M}{R}\right)_{cu} = \frac{1}{K}\left(\frac{S_{additive}}{M}\right)\left(\frac{M}{R}\right)_{cu} - \Delta \quad \text{(XXX)}$$

$$\cong \frac{1}{X^2}\left(aZ_A + bZ_B\right) u$$

The relative correction may then be estimated closely as follows:

$$\text{Relative correction} = \frac{\Delta}{(aZ_A + bZ_B)\ F\ (I_o)}$$

$$= \frac{\left[aZ_A\left\{\left(\ln\frac{I_{eff}}{I_o}\right)^2 - \left(\ln\frac{I_A}{I_o}\right)^2\right\} + bZ_B\left\{\left(\ln\frac{I_{eff}}{I_o}\right)^2 - \left(\ln\frac{I_B}{I_o}\right)^2\right\}}{u^4\ (aZ_A + bZ_B)}$$

Assume for simplicity that $I_{eff} = I_o$. Then:

$$\text{Relative correction} = \frac{+aZ_A\left(\ln\frac{I_A}{I_o}\right)^2 + bZ_B\left(\ln\frac{I_B}{I_o}\right)^2}{\left(2\ln\frac{2mv^2}{I_{eff}}\right)^4\ (aZ_A + bZ_B)}$$

One may now estimate the magnitude of this correction. Let I_H = 13 ev. and I_o = 67.15 and the energy be 340 Mev. Then for Benzene from Equation XXII:

$$\ln I_{eff}\ \text{Benzene} = \frac{6 \ln 13 + 36 \ln 67.15}{6 + 36}$$

$$I_{eff} = 53.1 \text{ ev.}$$

Then the relative correction is given by Equation XXXI. This correction is for the entire range of 340 Mev protons.

$$\text{Correction} = \frac{+ 6 \left(\ln \frac{13}{53.1}\right)^2 + 36 \left(\ln \frac{67.15}{53.1}\right)^2}{\left[2 \ln \frac{mv^2\ 340\ \text{Mev}}{I_{eff}}\right]^4 (6 + 36)}$$

$$= \frac{13.91}{[2 \times 9.09]^4\ (42)} = 2.94 \times 10^{-6}$$

Therefore the correction is negligible to the accuracy of this experiment.

Thus, it may be seen that the stopping power for a given element or compound is relatively independent of the energy at which it is measured and also independent of the amount of energy loss in the absorber as long as Bethe's Formula XI holds. With increasing energy, the relative stopping number as defined by Equation (VIII) increases with increasing Z but not as fast as Z itself as the I of the log factor also increases with Z. Thus the relative stopping power is a function of the particle velocity. The relative stopping power of carbon to copper as defined by Equation (X) decreases with an increasing incident proton energy where small

increments of the total energy are lost in the absorber. Therefore if a 340 Mev proton beam is incident on various samples, the thicker the sample, the higher will be the resulting relative stopping power obtained. We must therefore compare stopping powers at the same incident beam energy and with the same energy loss present in all samples. This was done by choosing sample thickness so as to reduce the beam energy from about 345 Mev to about 200 Mev. Corrections were applied to bring all samples to an exactly comparable basis. Below is shown a chart calculated from Aron's Tables (15) showing the trend. Note the lack of uniformity in the trends which indicate the limit of accuracy of the tables.

Table III

Energy loss in Absorber	S_C	S_H
350 - 300	0.25141	0.047732
350 - 250	0.25162	0.048447
350 - 200	0.25239	0.048576
350 - 150	0.25269	0.049310 Tabular error in (H_2)
350 - 100	0.25328	0.048912
350 - 0	0.25449	0.049275

From the above it is indicated that the correction is of the order of 1×10^{-5} in the stopping power for each Mev deviation from the 340 - 200 Mev chosen base energy. As the target energy reduction deviations from 200 Mev were of the order of 5 Mev or less, the corrections

were, in general, very small.

Using Equation (XIII) directly and values of I from Bakker and Segrè[9] the correction terms for the various elements used were calculated. The values below are stated in terms of change in S per Mev change in beam energy for thin targets. This correction remains practically constant throughout the range of this experiment. The energy at the front of the target is fixed by the cyclotron at about 340 Mev. The mean value of a given S between 340 and 200 Mev is desired. Thus one applies just one half the corrections listed to take into account variations in the energy of the emerging beam at the rear of the target, as the mean energy will change only half as much as a given change in the emerging beam energy. One half of this correction is to be added to targets which reduce the beam energy to a higher value than 200 Mev and subtracted from those which reduce the beam energy to below 200 Mev.

Table IV

Correction for	Correction S/Mev
Hydrogen	0.81×10^{-5}
Carbon	2.23
Nitrogen	2.35
Oxygen	2.46
Chlorine	2.65

As a practical definition of the energy interval 340 - 200 Mev an equivalent copper thickness of 53 grams-cm^{-2} of copper was chosen and all targets were corrected to this equivalent thickness.

III. EXPERIMENTAL

A. Experimental Definition of Range

The ranges were measured by use of the so called "Bragg curve" method. In this method the ionization energy loss of the proton beam in a thin ionization chamber is measured by collecting the electrons or positive ions from the ion pairs formed. As dE/dx increases rapidly as the residual range diminishes a plot of grams-cm^{-2} of copper vs. relative ionization loss in the ion chamber shows an increasing ionization loss until the point is reached where the protonshave a velocity comparable to that of the electrons in the outer shells of the target material. At that point ionization forming ion pairs no longer occurs and the curve drops sharply to zero. It is some point on this steep drop which gives the best range criterion. Various criteria were tested, including the extrapolated or tangent of steepest descent method, the point corresponding to approximately 0.5 of the maximum ordinate reached, and the point corresponding to the 0.8 point. Mather and Segrè[10] have shown by a "folding" operation that this point corresponds approximately to the mean range of the protons. That is, it corresponds to the center of an assumed gaussian distribution which is folded into the dE/dx curve. This later criterion has proved to be experimentally the best as far as giving repeatable results with the same sample as well as giving results which agree best among several samples.

B. Experimental Apparatus

The experimental arrangement is shown in Figures 1, 2, and 3. Figure 1 shows a schematic diagram of the cyclotron and cave area. The 340 Mev proton cyclotron beam was deflected or scattered out through the magnetic channel of the cyclotron. It was then collimated to 1/4 x 1/2 inch beam. A steering magnet bent the beam through approximately 20° and it then entered the cave area through a 1/2 inch diameter 40 inch long brass collimator.

The equipment in the cave is shown schematically in Figure 2. A photograph of the apparatus in position is shown in Figure 3. It consisted of, first, a front thin ionization chamber through which the proton beam entered the apparatus. This chamber served to indicate the magnitude of the current of entering protons. Immediately following this there was mounted a table on which could be placed 5 samples, any one of which could be placed in the beam at will. The samples were carefully milled solids or copper tanks for the liquids. Immediately following the samples was a set of shim absorbers which moved in conjunction with the samples. These served to even up any inequalities in the energy loss in the various absorbers so that all were approximately equal in energy loss.

Following this was an energy wheel with 12 slots containing step variations of copper of about 0.3 gram-cm^{-2} each. These were stamped with a circular die 4 in. in diameter from 12.5 mil selected copper and carefully weighed. After the wheel was located a set of 4 absorbers

working in a guillotine-like arrangement in such a way that any choice of these absorbers could be added or removed from the beam path by means of remote controls at a position outside of the shielding. Next in the beam path were a predetermined number of copper blocks of 4 in. square cross sections and varying thickness. Each block was milled plain, flat, and parallel to 0.2 mil and weighed to an accuracy of about 1 part in 50,000. Finally the rear ionization chamber was used to measure dE/dx near the end of the range.

C. Measurement Methods

1. The first method tried was that of using two separate integrators to integrate the beam current for a sufficient time to charge a known capacity. The total charge measured was read for both chambers and the ratio taken. To do this the beam had to be turned on to start the measurement and off to stop it. This was done initially by voice commands to the control room and later by a remote control cyclotron deflector on-off switch. It was observed that the beam was quite unsteady, both in energy and in amplitude during the start-up period. It was also observed that the electrically deflected beam was unsteady in energy, often taking jumps of 1/2 Mev or more within a few seconds. The scattered beam, on the other hand, showed no sudden energy jumps, but only gradual drifts over a period of many minutes. Therefore a current method was devised which could be used without turning off the beam and which did not require the larger total incident proton flux of the

deflected beam, thus enabling the use of the scattered beam. Switching devices for a charge integrating method were not seriously considered because of the uncertainties in the make and break charges left on the breaker points. It was felt that in view of the accuracy desired, such uncertainties could not be tolerated.

2. The first current method employed was essentially a null method. The potential on, say, the front chamber was reversed in sign and the current from both chambers was fed into a common lead and thence to an electrometer. Thus in one chamber the electrons were collected and in the other the positive ions were collected. The current read is the difference current and the null point will give some specific ordinate on a Bragg curve plot. By changingthe gas pressure in the chambers any ordinate could be selected. The method is extremely accurate and changes in sample thickness as small as 2-3 mg-cm^{-2} of copper can be measured. However, it was found experimentally that Bragg curves for different substances had maximum ordinates differing by as much as 10 percent due to multiple scattering, nuclear absorption, and small geometry changes. For this reason, readings taken in the manner indicated above gave results which did not correspond to any specific fixed fraction of the maximum ordinate. Runs made in this manner did not show the desired consistency and accuracy and were corrected by comparison with Bragg curves for the same substances to bring these results to values corresponding to 0.8 the maximum ordinate.

3. The second current method employed took all of the necessary points on the Bragg curve. During the first run in which current methods were employed to read the entire Bragg curve, the two currents from the ion chambers were recorded on tapes by two separate Leeds and Northrop Speedomax recorders. The ratio of these readings at any instant gave a point on the Bragg curve. The reading of these tapes proved to be a long and arduous task as it was necessary to compare the two traces millimeter by millimeter to obtain the traces at precisely the same time. A reader was devised and built to assist in positioning and holding the tape, but this still did not help much.

Following some work done by Michael Dazey, who had first suggested the idea and roughed it out on a Brown recorder, and with the assistance of Mr. Farnsworth and the electronics group, particularly G. Kilian and D. Merrill, a Leeds and Northrop Speedomax was converted into a ratio meter. The schematic diagram is shown in Figure 4. It should be noted that in order to have the instrument read a zero ratio on scale one must shunt out part of the slide wire itself and that is a fairly intricate operation and should be attempted only by someone who is throughly familiar with the recorder.

A second recorder hooked up to a supplementary thin ionization chamber in front of the apparatus in the beam was used to monitor the beam level. A side marking pen on each recorder hooked up in parallel as indicated in the diagram served to mark the time at which samples and

absorbers were changed. All equipment was designed with reasonable flexibility so that several methods of semi-automatic operation could be employed. Part of a Bragg curve ratio meter tape together with the beam monitor tape for this same period are shown in Figure 5. The linearity and consistency of the results agreed within 0.5 percent except for beam energy fluctuations.

By the use of 5 different control buttons 60 points could be measured on each of 5 separate Bragg curves without cutting off the beam entering the cave area. The controls were located in the counting area at the east side of the cyclotron.

In all cases, one of the 5 samples on the automatic sample changing table was copper. In practice, the sample thickness of all 5 samples on the table was adjusted by appropriate shims so that all samples plus shims had nearly the same stopping power. An appropriate wheel absorber and guillotine absorber was chosen and then with the beam on steady, ratio readings were taken of all samples. This procedure required about 20 seconds per sample or about 1-2/3 minutes for all five samples. During this short period, it was experimentally found that the beam energy drifted very little. After all five samples were run with a given wheel absorber, the wheel absorber was decreased one step, the procedure repeated. This went on until a sufficient number of points were obtained on the 5 Bragg curves to define completely the region near the end of the range, including the hump in the Bragg curve. The resulting curves of a typical set are shown in Figure 6.

The five experimental points corresponding to any given abscissa were taken within 1-2/3 minutes of each other. The temperatures were taken at the beginning and at the end of the run of each set of vessels. Temperatures were read to the nearest 0.02° on calibrated thermometers inserted in the top of the liquid tubes. If the liquids varied to any extent from room temperature before they were run, they were brought to room temperature by immersing the sample in its copper tube in a water bath at room temperature.

From the resulting Bragg curves the range was measured by the following procedure. The maximum height of the plotted curve was measured and 0.8 of this value was calculated. The abscissa of the point on the steep side of the Bragg curve whose ordinate was the 0.8 maximum height value was chosen as the range in copper in gms-cm^{-2}. The known values of the absorber thicknesses, the density equations, and the measured ranged were then used to set up a table as shown in Table V, from which S values were calculated. The table indicates only one typical set of data of part of one run. Most of the compounds and elements used were measured three or more times on separate runs. The errors shown are those estimated on the basis of the measurements involved. Note that the limiting error for the liquids occurs in the copper range measurements. This error is mostly due to small cyclotron energy fluctuations.

Proper corrections were applied to take into account the 0.316 gm-cm^{-2} of copper at each end of the liquid tubes. A similar

thickness of copper was added to the front of solid targets so as to maintain the energy at the front of all targets at the same value. From the total range in copper, 0.316 gm-cm^{-2} of copper was subtracted to give the "effective" range in copper for comparison purposes with other samples.

It should be noted that in general the copper values from one set to the next agree quite well. For example, values taken on 5 different days for the total range in copper are 92.137; 91.979; 92.151; 91.952; 92.151 gms-cm^{-2}. The last value is that corresponding to the run shown in Figure 6. The data of Table V which follows also corresponds to the Bragg curves shown in Figure 6.

D. Sample Preparation and Use

(a) General. The compounds measured were chosen to represent as nearly as possible within the scope of the experiment the types of variations of stopping power which might be expected. The elements hydrogen, nitrogen and oxygen could be measured in their pure state as liquids. The element carbon could be measured in the form of graphite. No diamonds of sufficient size to be measured were available. Compounds of chlorine were also chosen, although the element itself was not used because of its corrosive qualities.

The compounds selected were chosen to represent combinations of the elements H, C, N, O, and Cl. In order to qualify as a possible target it was required that the compound be obtainable in the highest purity,

Table V

Set I

July 9, 1951

Set	Target	Formula	Temp. (°C)	Density (gm-cm^{-3})	Tube Length (cm)	Sample (gm-cm^{-2})	Total Copper (gm-cm^{-2})	Equivalent Copper (gm-cm^{-2})	S_{cpd} Corrected
I	Chloroform	$CHCl_3$	20.63°	1.47637	31.740	46.860	36.924	54.911	2.19766
	Cyclohexane	C_6H_{12}	20.63°	0.77789	44.431	34.562	38.179	53.656	2.05346
	Benzene	C_6H_6	20.63°	0.87725	41.890	36.748	38.879	52.955	1.77082
	Carbon	C				39.917	38.211		
	Copper	Cu					91.835 (effective)		
Estimated Absolute Error (Liquids)			±0.02°	±0.00004	± 0.002	±0.002	±0.010	±0.015	±0.0005

stable enough so that it did not change during measurement, homogeneous in its samples and amenable to accurate sample thickness calculations. The compounds best fitting these criteria are liquids, as the measurements of temperature, density, and length of sample define the sample thickness and these can be given to a high degree of accuracy. Such compounds can often be purified readily by distillation and are homogeneous. Solids, on the other hand, proved to be very difficult, due mostly to inhomogeneities and lack of an ideal method to calculate sample thicknesses. Because of these difficulties with sample thickness such obviously interesting targets as methane, ethane, lithium compounds, salts in general, and most solids were discarded. The liquid containers were constructed from copper tubes of appropriate lengths. The ends of the tubes were faced off flat and parallel to 0.5 mil, and then 13.5 mil copper sheet of known thickness in gms-cm^{-2} was press fit in a hydraulic press onto each end by means of a retaining ring. Tests seemed to indicate that the ends were plane, flat, and parallel within 0.5 mil. Side tubes for draining and filling were provided at both ends. The lengths of the tubes were measured by a calibrated vernier caliper to an estimated $\pm$ 2 mil. Some of the tubes in the position in which they were used are shown in Figure 3.

The solid samples including the copper absorbers and graphite were ground plane flat and parallel to 0.2 mil. The dimension of the samples were measured by micrometers to 0.2 mil accuracy. The micrometers used were checked against standard gauge blocks. As most of the

samples were four inches square, this introduces a probable error of about one part in twenty thousand on each linear measurement made. The thickness of the copper blocks was uniform to 0.1 mil or better. Copper absorbers thinner than 3/16 in. could not be ground flat on their broad faces by a machine without warping. Therefore, these were checked for flatness and parallel sides and in some cases hand ground until uniform. In general it was found that the thin rolled copper was uniform to less than 0.1 mil in thickness over samples as large as 4 in. square. The 13.5 mil thick copper circular disks for the absorber wheel were punched out in an accurate punch press and any diameter was the same to 0.2 mil or better on any plate and also from plate to plate. The plates used were specially selected. The weights of the solid samples were obtained on an Ainsworth keyboard balance with a sensitivity of 0.2 milligram per pointer scale division. The heavier samples were weighed on a Radiation Laboratory balance with a sensitivity of 0.166 grams per pointer division. This balance and the weights were calibrated by the California State Bureau of Weights and Measures. By this means, all solid sample weights were obtained to an accuracy of better than one part in 10,000, and in general of the order of one part in twenty or thirty thousand.

(b) Polystyrene. Two different samples were prepared by cutting off and smoothing the ends of three inch diameter polystyrene rod. The polymerizing catalysts used were unknown but in the calculation have been assumed to be negligible.

(c) Polyethylene. The samples in this case were prepared by weighing large sheets of polyethylene and measuring accurately its area. From these measurements, the average sample thickness in gms-cm^{-2} was calculated. The large sheet was then cut into 32 pieces which were then stacked as the target. This target was run in the beam on different occasions. The results of four of these runs with the same target give the stopping power of CH_2 as 0.34449 ± 0.00008. (The error indicated here shows agreement between runs with the same sample.) On one occasion this target was split into two stacks of 16 pieces each. The results of these runs with short targets when corrected for the energy difference give the stopping power of CH_2 as 0.34005 and 0.34595. As the splitting into two targets may have been done in some selective manner, it is felt that the first values are better. A second short set of absorbers was prepared and run in a similar manner. The value obtained was 0.3421 when corrected for the energy difference. The error to be assigned on the basis of consistency of these results gives an answer 0.3432 ± 0.002. The error here assigned is due almost entirely to inability to measure the sample thickness with the desired degree of accuracy. Again in the case of polyethylene little is known concerning catalysts for the polymerization which may be present in the material. Plastic chemists have given assurance that these will be quite small.

(d) Liquid samples. The information available concerning the density and purity of various samples is given in a tabular form in

Table VII. That these things are important, is indicated by the following data in Table VI on the stopping power of n-hexane. As the dE/dx per gram-cm^{-2} is only a slowly varying function of atomic number small amounts of impurities of similar chemical structure will be relatively unimportant as long as the density is accurately known.

Table VI

Liquid Description	Density (18 °C)	Stopping Power
Solvent grade n-hexane	0.68185	2.1303
Purified grade n-hexane	0.66724	2.1435
Phillips 99 mol percent or better n-hexane	0.66123	2.1492

Determination of Densities. Equations exist (calculated from the best available experimental data on the basis of least squares) for the determination of the densities of most of the liquids used[17]. The accuracy quoted in this reference are of the order of one part in one thousand or better. However, it was found experimentally that the densities obtained by use of these equations did not give sufficient accuracy in some cases and in others equations did not exist. For these reasons it was considered necessary to measure the densities experimentally. A pycnometer method was chosen. A 50 cc. volumetric Pyrex flask with a tapered ground glass joint was chosen and fitted with a tapered top containing a capillary tube. It was soon found in preliminary tests that the more volatile of the liquids were still evaporating enough during

the weighing to effect the results. For this reason an extra cap was added effectively shutting off the capillary and the entire top of the vessel from the outside air. A tare flask with the same extra tops was used in the weighing.

A constant temperature bath was set up using an electrical spade heater and controlling the temperature to within 0.02 °C by use of a Fenwal Regulator. The bath was maintained at a temperature above room temperature in order that the liquid always contract during the weighing process. The temperature was taken on a 0.1° thermometer calibrated by the Bureau of Standards. Accurate estimates could be made to the nearest 0.02°. The volume of the vessel was determined by weighing distilled water samples and determining from the I.C.T. the density of water at the bath temperature. The volume of the flask was determined as a function of temperature by a series of more than 10 measurements. The accuracy based on internal consistancy was found to be ± 1 Part/ 52,000.

To measure a liquid density the pycnometer containing the liquid was immersed in the temperature bath for several hours until the liquid had reached the known bath temperature. The tare was also immersed briefly just before both were removed. The liquid level was checked shortly before removal from the bath. If low, it was replenished by means of a micropipette. If too high, the excess was blotted off with a Kleenex. The vessels were then capped with the extra tops and

removed from the bath. Both vessels were thoroughly and quickly wiped dry and they were then weighed. Reweighing after 5 or 10 minutes indicated that any moisture remaining on the outside of the vessels and not cancelled by use of the tare flask was less than one part in about 100,000

Several of the liquids, notably styrene, dichlorodiethyl ether, trichloroethylene, tetrachloroethylene, and ββ' dichlorodiethylether did not have published temperature-density relationships. These were measured and fitted by a linear temperature correction. The densities were taken for at least 3 temperatures to make this determination. In the case where these relations already existed, the temperature terms given in the literature were used in conjunction with the experimental values determined at two or more points, to give a density relationship which was finally used. On the basis of rechecks, agreement with the literature values, and internal agreement of measurements, it is felt that the density can be reported at any given temperature to an accuracy of about 1 part in 20,000.

The densities finally used are given in Table VII. The base temperature used was 18 °C. Corrections are from that value. The values given include temperature corrections based on Bureau of Standards calibration and corrections for buoyancy effects during the weighing process. All weights used were calibrated and the corrections were employed in the calculations. The values given quoted from the International Critical Tables are calculated from the equations found there and are reportedly accurate with a limit of 0.0002 to 0.0005 in most cases.

Table VII

Liquid Target Data

Chemical Sources

B.A. = Baker analyzed
C.B. = Coleman and Bell
C.D. = Caldow
E.A. = Eimer and Amend
E.K.W. = Eastman Kodak White Label (99 + percent)
E.K.Y. = Eastman Kodak Yellow Label (96 + percent)
P = Phillips Petroleum (99 + percent)
S = Shell Chemical

Legend

C.P. = Chemically pure
A.C.S. = Meets A.C.S. standards
I.C.T. = International Critical Tables
(all I.C.T. values based on equations given in that reference)
(2), (3), etc. number of different lots used from the same source.

Compound	No. of Samples	Fractional Distillation	B.P. (Measured)	Density (18 °C) (A) Measured	(B) Table	(A-B)	Source
Benzene	3	yes	79.5°-80.0°	0.88006	0.8809	-0.0008	B.A.-A.C.S.-C.P. (2) C.B.-A.C.S.-C.P.
Toluene	2	yes	110°-111°	0.86764	0.8675	+0.0001	B.A.-A.C.S. Reagent (2)
m-xylene	2	yes	138°-139°	0.86458	0.8661	-0.0015	B.A.-A.C.S. Reagent (2)
n-pentane	1	no		0.62858	0.6282	+0.0003	P - 99 percent
n-hexane	1	no		0.66122	0.6613	-0.0001	P - 99 percent
n-heptane	1	no		0.68552	0.6853	+0.0002	P - 99 percent
cyclohexane	2	yes	79.2°-80.2°	0.78032	0.7808	-0.0005	C.D. - 99 percent

Compound	No. of Samples	Fractional Distillation	B.P. (Measured)	Density (18 °C) (A) Measured	(B) Table	(A-B)	Source
Styrene	3	yes	(vacuum distilled)	0.90949 (variable)	not known		S.
Carbon Tetrachloride	3	yes	75.5°-76.0°	1.59580	1.5979	-0.0021	B.A.-C.P. (3)
Chloroform	2	yes	59.5°-60.0°	1.48132	1.4928	-0.0115	B.A.-A.C.S.-C.P. (2)
Chlorobenzene	1	yes	128°-129°	1.10863	1.1085	+0.0001	E.K.-W
O-Dichlorobenzene	1	no		1.30777	1.3048	+0.0003	E.K.-Y.
β-β'-Dichloro diethyl ether	1	no		1.22001	1.222,	-0.0020	E.K.-W
1,2 Dichloro ethylene	1	yes	81.2°-82.0°	1.25588	1.2566	-0.0010	B.A.-Tech.
Trichloroethylene	1	no		1.46698	1.4556 (25/4 or) 1.4672	-0.0002	E.K.-W
Tetrachloro ethylene	1	no		1.62363	1.6183	+0.0053	E.K.-W.
Methyl Alcohol	3	yes	64°-65°	0.80108	0.7935	+0.0074	B.A.-A.C.S. Reagent (1) -A.C.S.-C.P. Abs. (2)

Compound	No. of Samples	Fractional Distillation	B.P. (Measured)	Density (18 °C) (A) Measured	(B) Table	(A-B)	Source
Ethyl Alcohol	3	absolute	Distilled (1) from Benzene (2) from drying agent	0.79309	0.7911	+0.002	B.A.-others
n-Propyl Alcohol	1	no		0.80595	0.8044 (at 20/4)		E.W.-W.
n-Butyl Alcohol	1	yes	116°-118°	0.81140	0.8112	+0.0002	B.A.-C.P.
Glycerine	1	no		1.24899	1.2625	-0.0135	B.A.-A.C.S.-C.P.
Acetone	3	yes	56°-56.2°	0.79227	0.7923	0.0000	B.A.-A.C.S.-C.P. (3)
Diethyl Ether	2	yes	34.4°	0.71613	0.7158	+0.0003	B.A.-A.C.S.-C.P. B.A.-A.C.S.-Reagent
Pyridine	2	yes	113°-114°	0.97888	0.9852	-0.0063	B.A. Reagent B.A. Purified
Nitro-benzene	1	yes	208.5°-211°	1.20514	1.2052	-0.0001	E.K.-W.
Analine	2	yes	183°-186°	1.02320	1.0234	-0.0002	B.A.-A.C.S. Reagent E.A.
Water	20	yes	Assumed as basis for all densities				

Density equations as a function of temperature were obtained during the experiment for a number of compounds. These could not be found in the literature. In other cases the expansion coefficients as a function of temperature were obtained from the International Critical Tables.

Table VIII

	Density Equations (t in °C)
Styrene	$\rho_{to} = 0.909486 + (0.8965)(18-t_1)(10^{-3})$
Trichloroethylene	$\rho_t^o = 1.466977 + (1.6733)(18-t_1)(10^{-3})$
Tetrachloroethylene	$\rho_t^o = 1.623627 + (1.610)(18-t_1)(10^{-3})$
O-dichlorobenzene	$\rho_t^o = 1.307767 + (1.108)(18-t_1)(10^{-3})$
BB' dichlorodiethylether	$\rho_t^o = 1.220014 + (1.145)(18-t_1)(10^{-3})$

(e) Carbon (Graphite). The graphite used was pile grade graphite. At least 5 different samples of two grades of porousness were used. A typical analysis of a sample of grade as given by the National Carbon Company follows:

C-18 Carbon (Max Impurities)	
Ash	0.110 %
Ca	0.039
Fe	0.002
Va	0.006
Tu	0.002
	0.159 %

Great pains were taken in the cutting of samples. Figure 7 shows a projected sketch of two such samples cut from a piece 8 x 20 x 24 inches.

By means of cuts taken from the center of large pieces it was hoped to reduce any inhomogeneities in density. On two sets of such samples the beam was passed through the samples along all three of the principal axes. The result along these axes differed somewhat. In fact, in passing through the same two blocks at points indicated by B and C or by D and E in Fig. 7, the results differed by an easily detectable amount. The final result used is that obtained by averaging all directions on both of the two sample sets used.

The error to be attributed to the carbon results must for the most part, be assigned to calculation of the proper sample thickness. There are two main reasons for this uncertainty. First, there no doubt exist inhomogeneities in the density of the samples. The carbon blocks molded or extruded may present a different effective density to the penetrating protons than the overall average density obtained by weighing and measuring the entire sample.

Second, the carbon atoms in graphite are known to be linked into benzene like rings and sets of rings[18,19]. As such, they lie in flat planes and small crystals. If these crystals tend to be aligned by the method of formation for the blocks, then there might be effectively more atoms and hence molecules presented to the beam in one direction than in another over limited volumes. Another effect may be that this same orientation of crystals may present a larger proportion of the electrons which are more or less free to move about the benzene like rings

or it may present a larger proportion of the electrons which help to bind the carbons to one another.

In a typical sample the beam was passed through the sample in the directions shown by the lettered arrows A, B, C, D of Figure 7.

The results of runs on one set of samples are given below. Note that the values for the D and E directions were obtained by turning Block 1 and Block 2 through 90° about their long axis, and passing the beam through both blocks at the same time.

Values of S	Average	Average
A_1 = 0.244820 A_2 = 0.244206	0.244513	
B = 0.244883 C = 0.245199	0.245041	0.245153
D = 0.245195 E = 0.246003	0.245599	

The results of several runs with three different samples give the value shown in the arrangement above. It will be noted that the maximum deviation in the sample is about 1 part in 250. In the case of one sample this was even larger and 1.7 parts in 250. This second sample gave an average value in all three directions of 0.24574.

(f) Styrene. The styrene samples procured were distilled free of polymerization inhibitors under a high vacuum and fractionation so as to insure a negligible amount of impurity. The density of the

sample as a function of temperature was measured just before each run and checked with the expansion coefficient worked out experimentally earlier. As a function of long periods of time the density of the styrene changed as it slowly polymerized under the action of heat and light. It was found that polystyrene could be kept in the dark at about 35 °F. for several months with very little polymerization.

(g) Hydrogen. The stopping power of liquid hydrogen was measured in a liquid hydrogen target originally designed by Dr. Vincent Peterson[20] during the course of a meson production experiment. It was substantially redesigned and tested by Charles Godfrey of this laboratory. The hydrogen container consisted of a horizontal tube 36.322 inches long and three inches in diameter connected at the center of the top to a reservoir containing about 6 liters of hydrogen in a column 41-1/2 in. high. In operation the entire target was placed on a movable table in the cave. Its operation could be controlled from outside of the cave. In this way, the hydrogen column or an equivalent amount of copper could be placed in the beam without shutting off the beam. The empty target was first run in comparison to an equivalent copper absorber. The target was then filled with hydrogen and allowed to come to a steady state condition. This filled target was then run and compared with an equivalent copper absorber. From these measurements the equivalent copper absorber to the actual hydrogen present was calculated. The length of the target was measured accurately and a small correction of 0.062 in. was applied

to correct for the curvature of the slightly flattened tube ends and the resulting variation in sample thickness. The value for the density of liquid hydrogen at the boiling point as a function of pressure was taken from data given by the Bureau of Standards.[21,22] The pressure was read by a barometer. As there was a check valve in the system a test was made using a manometer to determine whether or not any pressure differential existed between the inside of the hydrogen vessel and the outside. No detectable pressure difference was found to exist.

Another worry was possible presence of bubbles in the tube at the time of measurement. The rate of evaporation of the hydrogen from the vessel was measured as a function of time. This indicates, first, that part of the loss is due to heat conducted down through the metal from the top and part to loss by radiation or conduction out through the horizontal tube. This was to be expected as the vacuum was maintained at better than 2×10^{-5} mm of mercury at all times and the entire horizontal tube was surrounded by a heat shield.

The loss may be extrapolated downward to the top of the horizontal tube and gives a loss at that point of about 1/12 cc per second of liquid or 4.45 cc/sec. of gaseous hydrogen. If the average bubble size is chosen as having a radius of 0.1 centimeter, use of Stoke's law will give a value for the rise of bubbles in the solution of about 1100 centimeters per second. As the mean distance from the bottom of the container is only 1-1/2 inches, it is clear that Stoke's law giving a

terminal velocity will not apply here. If it is assumed that the bubbles rise under a force due to the density difference between liquid and gas and that the rising gas bubble can be represented by an equal mass of hydrogen liquid moving downward, we obtain values for the bubble rise velocity at the center of the tube 1-1/2 inches from the bottom of about 68 cm/sec. This is essentially a free fall calculation and neglects the viscosity of liquid hydrogen. (The coefficient of viscosity of liquid hydrogen at its boiling point is 0.00013 Poise and may be contrasted with that of water of 0.010087 Poise at room temperature.) Let us assume that due to viscosity the velocity is reduced to 50 cm/sec. which cannot be high by more than a factor of 2. (The Stoke's velocity calculated and measured for bubbles of the same size in water is about 10 cm/sec.) Of all of the hydrogen boiling out, about 1/2 will come from the side and upper walls and therefore will not cross the beam path. If it be assumed that all of the separate bubbles can be grouped into a flow through an imaginary pipe perpendicular to the beam and that the gas in this pipe behaves like an incompressible fluid, a cross sectional area of an equivalent pipe may be calculated. If the width of the pipe in the horizontal direction perpendicular to the beam is two inches (corresponding to a rough measure of beam width) the thickness of the pipe is 8.8×10^{-3} cm. This is equivalent to a loss in effective length of hydrogen of 6.2×10^{-4} gram/cm^2. As the total target thickness is 6.549 gms/cm^2, the error due to bubbles is of the order of one part in 10,000 and is negligible.

There is one other possible error. The density calculated is that for normal hydrogen. The normal mixture is seventy-five percent ortho and twenty-five percent para hydrogen. This is the mixture percentage first resulting when the hydrogen is condensed. The equilibrium mixture at the boiling point of hydrogen (20.4° K) is 99.8 percent para hydrogen. The density of normal hydrogen is 0.07099 at 20.38° K. At the same temperature the density of para hydrogen is 0.07065 which differs by 0.48 percent from the normal mixture. The conversion from normal to the para form occurs only slowly without special catalysts.[22] For this reason, the measurements were made as soon as possible after the preparation of the sample. All measurements were made within seven hours of the end of the preparation.

It may be noted that some of the boiling of the hydrogen must be attributed to this change in state and its attendant release of heat energy. This boiling should occur for the most part at the walls due to the need for a catalyst to promote the reaction.

The calculated stopping power for hydrogen was based on the density at the boiling point, which in turn is fixed by the atmospheric pressure. The Bureau of Standards measurements were accepted as correct.[21,22] These give: Vapour pressure of Liquid H_2 $\log_{10}$ (mm hg) = $4.6633 - \frac{44.7291}{T} + 0.02023\ T$.

Volume of Liquid Normal H_2/mole = $V(cm^3/mole) = 24.747 - 0.08005\ T + 0.012716\ T^2$. These equations and the measurements of ranges taken, when corrected for the two small energy loss in the hydrogen and tube contraction (the target reduces the beam energy only to 290 Mev) give the stopping power of molecular hydrogen.

(h) Nitrogen and Oxygen. These liquified gases were measured in a special copper container. (See Figure 8.) The inner liquid container was one of the carefully made liquid target tubes with its flat ends and calibrated end windows. Its length at room temperature was 44.4314 cm. In order to keep pressure or vacuum from the ends of the tube the ends were sealed by small chambers which were open to dry nitrogen or oxygen so as to prevent water vapor condensing on the chamber ends. The whole was then jacketed by an intermediate jacket and both inner and intermediate chambers were filled with the liquid gas. Surrounding the double inner jacket was an outer vacuum jacket. By this means, the center measuring chamber vented only at three places at the top would be free of bubbles as the two concentric inner and intermediate chambers would act like a double boiler, the bubbling occuring in the intermediate chamber only, as long as any liquid remains in it. Equations given in the International Critical Tables were used for the calculation of the density at the boiling point as a function of the measured pressure. The results were corrected to the proper energy interval (200-340 Mev) and for contraction of the tube length.

E. Checks of Method and Procedure

(a) Liquids - Purity, Density. The errors quoted in the tabulated experimental results are based on the agreement of runs done on different days and often with different samples. They are therefore an indication of the consistency of the runs as regards the method and the apparatus used. They give no absolute indication of the accuracy as far

as sample purity is concerned. As indicated in Table VII, more than one sample was used when it was available. That this may be important is born out by the results obtained by various samples of normal hexane as indicated in Table VI. It was predicted that the final result for the pure n-hexane should be near 2.49 from consideration of agreement between various compounds.

Purity of the compounds was insured by selection of highly pure (C.P. or better) chemicals, redistillation in many cases, boiling point, density, rechecks between samples from various sources, and agreement among different compounds.

The densities measured agree quite well in most cases with the literature and for those that deviate appreciably the deviation is in the correct direction to be explained by a small amount of impurity of a reasonable nature (i.e. water, etc.).

(b) Liquid Target Lengths. Runs made with benzene in all eight of the liquid containers of different lengths used bear out the accuracy of the measurement of target tube length and indicate the agreement between this method and expected theoretical values.

In Figure 9 the beam energy at the back of the target (the beam energy at the front was always approximately 340 Mev) is plotted as the abscissa against the stopping power of benzene. Curve A is calculated theoretically from Aron's tables assuming strict additivity of the stopping powers of carbon and hydrogen. Curve B is the experimental curve obtained. It will be noted that the values of Curve B are

definitely and uniformly lower, but that the slope is in excellent agreement in both graphs. This serves as a check on the various containers and on the relative location of these containers in the beam. It is worth while noting that the two high values marked with a + are from a different benzene sample than the other values.

(c) Geometry of Liquid Targets in Beam. Another check run was that of varying the placement of the liquid target on the movable table. Figure 10 shows two Bragg curves taken of the same target (Trichloroethylene) on the same day during different runs. Curve A resulted when the target was placed with its rear face within one inch of the rotating wheel assembly (see Figure 2 or 3). Curve B resulted when the target was moved forward toward the cyclotron snout a distance of 8 in. The loss in height in curve B indicates clearly that much of the beam is being scattered out and lost. However, it shows that the beam is lost from both the rear absorbers and the rear ionization chamber. The resulting 0.8 of maximum height points on the Bragg curves agree extremely well and the resulting stopping powers obtained are $S_A = 2.4492$ and $S_B = 2.4483$. Note that the 0.074 gm-cm^{-2} difference in the amount of copper necessary to stop the beam is made up by a similar shift in the range of the beam in copper. Thus the difference in equivalent copper is 0.019 gm-cm^{-2}, about one probable error. This shows rather conclusively that target position in the geometry used has a negligible effect. In no case was the geometry changed in as radical a manner as in this test.

(d) Possible Effects of Tube Walls. Photographs taken at various points of the apparatus with x-ray film in the beam showed clearly that a negligible part of the beam was being absorbed by the chamber walls or other parts of the apparatus. This was further verified by another test. The solid polystyrene target was run with nothing surrounding it. Then the same target was surrounded by a copper tube similar in diameter and wall thickness to those used in the liquid tubes. End windows were taped on and the same target was run again. The stopping power for polystyrene obtained in the two cases was:

No tube outside	$S_{C_8H_8}$	2.3597
Cu tube outside	$S_{C_8H_8}$	2.3587

These two results disagree by less than two probable errors.

(e) Beam Current Effects. Tests were run on the behavior of the ratio meter as a function of beam current through the apparatus. The same set of samples was run with the beam at its normal level, then with it at one half of its normal level, and then something above its normal level. The results for a single compound, polystyrene, are given below.

Table X

Beam Current (Ion Chamber)	$S_{Polystyrene}$
0.25×10^{-8}	2.3744
0.20	2.3597
0.10	2.3573

This test indicates that with the ratio meter the beam current level must be maintained in the proper region. In actual fact the meter can be regulated by the variable resistances indicated in Figure 4 so that it will function properly on quite a wide range of beam currents. However, once a run is started the beam level must be maintained at that level within about 20 percent fluctuations if good results are to be obtained.

(f) Ionization Chambers. At the beginning of each run the ionization chambers were checked to see that they behaved in a linear fashion as a function of collecting voltage. They gave consistently the same results within 0.2 percent over a voltage plateau of from 1000 volts to 2000 volts. The sensitive volume of the chambers is two inch deep and in general were filled to just above atmospheric pressure with pure argon. Previous experiments[23] by others of this group have shown that these chambers do not exhibit saturation until the beam current levels become at least a factor of ten larger than those used in this experiment.

(g) Ratio Meter. The plots of the Bragg curves involved in finding the range, were obtained from readings given by the so-called "ratio meter". This resulted in a set of readings on a Leeds and Northrup Speedomax Recorder chart. There were 100 divisions on this chart. Linearity checks and duplication of the same point in any given Bragg curve indicated that this tape could be accurately read to $\pm$ 0.1 divisions. Drift of the zero on the instrument was small and was checked

frequently.

At points on the steep slope of the Bragg curve near the 0.8 maximum height point a change in absorber thickness of 0.3 grams of copper causes a change of about 10 divisons of the Recorder chart. Therefore the reading error stated in terms of copper absorber is about 3 milligrams per square centimeter of copper. Small drifts in energy in the cyclotron beam cause fluctuations of any given point on the steep slope of the Bragg curve by an amount equivalent to an estimated 0.5 of one division on the chart or 15 milligrams per square centimeter of copper. This variation is reduced somewhat by plotting and drawing the best smooth curve through the experimental points. Except for certain solid samples where density is not well determined, the beam fluctuations form the limiting error of the experiment.

IV. TABULATION OF RESULTS

A. Typical Sets of Data

In Table XI are listed typical sets of data for the various materials tested. These were taken at random from their groups of 5 samples which were run at the same time. In order to condense the table the accompanying range in copper is not given, but only the equivalent copper.

Table XI

Typical Data of Materials Measured

Carbon-Hydrogen

Target	Formula	Sample $gm\text{-}cm^{-2}$	Equivalent Copper-$gm\text{-}cm^{-2}$
Hydrogen	H	6.5291	19.309
Carbon	C	39.9172	52.257
Benzene	C_6H_6	37.7846	52.986
Toluene	C_7H_8	36.3275	52.995
Xylene	C_8H_{10}	36.1558	53.170
n Pentane	C_5H_{12}	31.8073	50.606
n Hexane	C_6H_{14}	33.291	52.775
n Neptane	C_7H_{16}	34.751	54.941
Cyclohexane	C_6H_{12}	34.5626	53.656
Styrene	C_8H_8	38.0980	54.859
Polystyrene	$(C_8H_8)_n$	38.2169	54.932
Polyethylene	$(CH_2)_n$	35.5637	55.514

See Table XII for results.

Carbon-Hydrogen-Oxygen

Target	Formula	Sample gm-cm^{-2}	Equivalent Copper-gm-cm^{-2}
Oxygen	O	50.785	64.406
Water	H_2O	35.4706	51.794
Methyl Alcohol	CH_3OH	35.5693	53.242
Ethyl Alcohol	C_2H_5OH	35.1478	53.273
n-Propyl Alcohol	C_3H_7OH	33.756	51.469
n-Butyl Alcohol	C_4H_9OH	34.0105	52.061
Glycerine	$C_3H_5(OH)_3$	36.3932	52.238
Acetone	C_3H_6O	35.2301	51.943
Diethyl Ether	$C_2H_5OC_2H_5$	36.3811	55.653
β,β', Dichloro-diethylether	ClC_2H_4-O-C_2H_4Cl	43.3317	56.970

See Table XIV for results.

Carbon-Hydrogen-Chlorine

Carbontetra chloride	CCl_4	46.4647	53.482
Chloroform	$CHCl_3$	46.9203	54.912
Chlorobenzene	C_6H_5Cl	39.3842	52.403
o-Dichloro-benzene	$C_6H_4Cl_2$	41.5100	52.796
Trichloro-ethylene	CCl_2=CHCl	46.4446	54.921
Tetrachloro-ethylene	CCl_2=CCl_2	47.2052	54.777
1,2 Dichloro-ethane	C_2H_4Cl	36.6291	46.455

See Table XIII for results.

Carbon-Hydrogen-Nitrogen

Target	Formula	Sample $gm\text{-}cm^{-2}$	Equivalent Copper-$gm\text{-}cm^{-2}$
Nitrogen	N	35.955	46.255
Analine	$C_6H_5NH_2$	38.2193	55.865
Pyridine	C_5H_5N	37.1945	52.745
Nitrobenzene	$C_6H_5NO_2$	38.2301	52.253

See Table XV for results.

Table XII

Carbon-Hydrogen Results

Compound	Formula	Runs	Stopping Power**
Hydrogen	H	3 (same day)	0.04721±0.0002(est.)
Carbon	C	18	0.2455 ±0.0005(est.)
Benzene	C_6H_6	11 + 4*	1.77326±0.00037
Toluene	C_7H_8	1 + 2*	2.11442±0.0013
Xylene	C_8H_{10}	3 + 2*	2.45605±0.00011
n-Pentane	C_5H_{12}	5 + 2*	1.80715±0.00053
n-Hexane	C_6H_{14}	1	2.14919±0.001(est.)
n-Heptane	C_7H_{16}	3	2.49121±0.00055
Cyclohexane	C_6H_{12}	4 + 3*	2.05346±0.00042
Styrene	C_8H_8	4 + 1*	2.36185±0.00083
Polystyrene	$(C_8H_8)_n$	5 + 4*	2.35703±0.0009
Polyethylene	$(CH_2)_n$	5 +	0.34499±0.00008

* Runs made by method (2) (single point current method) and corrected to 0.8 maximum height values from Bragg curves).

** All errors indicated are those based on internal consistency of runs for any given compound.

Table XIII

Carbon-Hydrogen-Chlorine Results

Compound	Formula	Runs	Stopping Power**
Carbon Tetrachloride	CCl_4	3 + 2*	2.73474±0.00043
Chloroform	$CHCl_3$	5 + 2*	2.20037±0.00044
1,2 Dichloro-ethane	$C_2Cl_2H_4$	1	1.976 ±0.0039(est.)
Chlorobenzene	C_6H_5Cl	2 + 2*	2.35518±0.00031
Orthodichloro-benzene	$C_6H_4Cl_2$	1	2.94200±0.001(est.)
Trichloro-ethylene	C_2Cl_3H	3 + 2*	2.44378±0.00062
Tetrachloro-ethylene	C_2Cl_4	1 + 2*	3.02714±0.0004
β,β', Dichloro-diethylether	$C_4Cl_2H_8O$	1 + 1*	2.95285±0.00049

* Runs made by method (2) (single point current method) and corrected to 0.8 maximum height values from Bragg curves.

** All errors indicated are those based on internal consistency of runs for any given compound.

Table XIV

Carbon-Hydrogen-Oxygen Results

Compound	Formula	Runs	Stopping Power**
Oxygen (O_2)	O	2 (same day)	0.3188 ±0.0003(est.)
Water	H_2O	1 + 2*	0.41411±0.000083
Diethyl ether	$(C_2H_5)_2O$	1 + 1*	1.78457±0.00048
Methyl Alcohol	CH_3OH	1	0.754498±0.0005(est.)
Ethyl Alcohol	C_2H_5OH	3 + 3*	1.09875±0.00014
n-Propyl Alcohol	C_3H_7OH	1	1.44149±0.0005(est.)
n-Butyl Alcohol	C_4H_9OH	1*	1.78460±0.001(est.)
Glycerine	$C_3H_5(OH)_3$	1 + 2*	2.07896±0.00066
Acetone	C_3H_6O	2 + 2*	1.34920±0.00034

* As shown above.

** As shown above.

Table XV

Carbon-Hydrogen-Nitrogen Results

Compound	Formula	Runs	Stopping Power**
Nitrogen	N	3 (same day)	0.2837 ±0.0001(est.)
Nitrobenzene	$C_6H_5NO_2$	2 + 2*	2.64777±0.00031
Analine	$C_6H_5NH_2$	1	2.10075±0.001(est.)
Pyridine	C_5H_5N	3 + 2*	1.76469±0.00047

* Runs made by method (2) (single point current method) and corrected to 0.8 maximum height values from Bragg curves.

** All errors indicated are those based on internal consistency of runs for any given compound.

V. ANALYSIS OF RESULTS

A. Carbon - Hydrogen

The liquid results being the least subject to error should give the best indications of deviations from additivity. If it be assumed that the stopping power is strictly an additive function of the elements present we may set down a series of equations for the compounds involved and using the now determined experimental values obtain a least squares solution for values of the stopping powers for carbon and hydrogen. Standard methods for calculation of least squares solutions and errors were used. Styrene, polystyrene, and Polyethylene were omitted from the equations below as their S value could not be determined experimentally as well as the rest.

Table XVI

Equations	Exp.-calc. = v
$6\ S_C + 6\ S_H = 1.77326$	$+ 125 \times 10^{-5}$
$7\ S_C + 8\ S_H = 2.11442$	$- 2$
$8\ S_C + 10\ S_H = 2.45605$	$- 81$
$5\ S_C + 12\ S_H = 1.80715$	$+ 82$
$6\ S_C + 14\ S_H = 2.14919$	$+ 43$
$7\ S_C + 16\ S_H = 2.49121$	$- 3$
$6\ S_C + 12\ S_H = 2.05331$	$- 126$
	$\Sigma v^2 = 4.665 \times 10^{-6}$

These give:

$$S_C = 0.24824 \pm 0.00012$$

$$S_H = 0.047094 \pm 0.000068$$

It will be noted at once that the agreement is very good. The C-H value given above corresponds to the circled point of Fig. 11 at the coordinates given above for S_C and S_H

The equations, as shown on the preceding page, stated in their first form on a purely additive basis may be plotted in a very instructive manner. If S_C and S_H are treated as unknowns x and y and S_C is plotted as the abscissa and S_H as the ordinate, then each equation, shown on the preceding page, becomes a straight line on the graph. Any point on a given line representing one compound satisfies the experimental determined value for the stopping power of that particular compound. Thus, if two lines cross, the crossing point determines the value of S_C and S_H which satisfies both compounds. The seven equations are plotted on such a graph in Figure 11. Note the similarity of the slopes of the lines. This makes it hard to determine a unique answer accurately.

This indicates that there appears to be a real difference in the stopping power of hydrogen in aromatic unsaturated as compared to straight chain saturated. The values obtained from the graph are $S_{Ha} = 0.0497$, $S_{HS} = 0.0479$ or about 3.7 percent different. The width of the line is roughly the magnitude of the probable error in a given determination.

The graph also shows that there is a small variation in S_C and it gives values of $S_{Ca} = 0.2458$, $S_{CS} = 0.2464$ or about 0.24 percent.

Now assume that there exists a factor present in each organic double bond which makes the stopping power of unsaturated hydrocarbons differ from saturated hydrocarbons.

On this basis the equations of the last couple of pages have been revised as follows:

Table XVII

Equations	Exp.-calc. = v
$6\ S_c + 6\ S_H + 3\ D = 1.77326$	+ 85
$7\ S_c + 8\ S_H + 3\ D = 2.11442$	- 16
$8\ S_c + 10\ S_H + 3\ D = 2.45605$	- 70
$5\ S_c + 12\ S_H = 1.80715$	+ 14
$6\ S_c + 14\ S_H = 2.14919$	+ 2
$7\ S_c + 16\ S_H = 2.49121$	- 14
$6\ S_c + 12\ S_H = 2.05331$	+ 29
	$\Sigma v^2 = 1.3618 \times 10^{-6}$

These give:

$S_c = 0.24601 \pm 0.00057$

$S_H = 0.04808 \pm 0.00022$

$S_D = 0.00262 \pm 0.00057$

The double bond assumption here is equivalent to a choice of two types of carbon as there is one double bond for each two aromatic carbon atoms. The double bond factor as calculated is about 4.6 times the probable error. It is also equivalent to a single ring factor three times as large as the double bond factor. This may indicate a difference of the type assumed but it is certainly doubtful. All of the probable errors are higher. It does tend to indicate that the basic assumption of this calculation may not be too good. The 3D factor was subtracted

from the aromatic stopping powers and the results plotted in Figure 12. The graph again shows that it is hard to get a good fit with this assumption.

For a third calculation assume that there exist two types of hydrogen, one in saturated compounds (H_S) and one in unsaturated (H_a). This results in the following equations.

Table XVIII

Equations	Exp.-calc. = ν
$6\ S_c + 6\ S_{Ha} = 1.77326$	-8×10^{-5}
$7\ S_c + 5\ S_{Ha} + 3\ S_{HS} = 2.11442$	-13
$8\ S_c + 4\ S_{Ha} + 6\ S_{HS} = 2.45605$	+28
$5\ S_c + 12\ S_{HS} = 1.80715$	+30
$6\ S_c + 14\ S_H = 2.14919$	+ 8
$7\ S_c + 16\ S_{HS} = 2.49121$	-17
$6\ S_c + 12\ S_{HS} = 2.05331$	-28
	$\Sigma \nu^2 = 0.27 \times 10^{-6}$

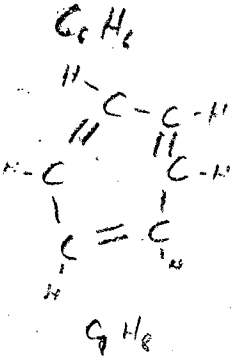

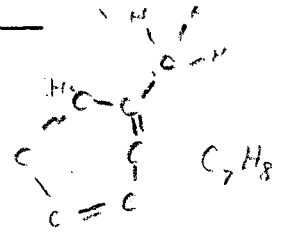

This assumption gives results:

$S_c = 0.24676 \pm 0.00013$

$S_{Ha} = 0.048806 \pm 0.00015$

$S_{HS} = 0.047758 \pm 0.000060$

The difference in stopping of the two hydrogens is 0.001048 or about 7 times the larger probable error. The magnitude of the probable errors is also lower here indicating somewhat better agreement. The difference in the stopping powers of the two types of hydrogen is about 1.9 percent with the aromatic hydrogen being the more effective.

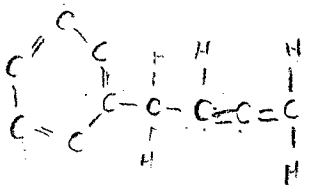

A study of the aromatic compounds shows that toluene and xylene contain saturated groups as well as unsaturated rings. Thus, even though the agreement shown by the graph of Figure 11 is excellent, the real effect may still be hidden. Since it is precisely these methyl groups which cause the difference in slopes, there should be good agreement after a recalculation. From the graph one can read off the aliphatic saturated values for S_{CS} and S_{HS}, put these values into the experimental results for the aromatics to subtract off the methyl radicals, and solve for new values for the unsaturated stopping powers (S_{Ca} and S_{Ha}). A better method is to use least squares solution of the seven equations rewritten as below.

Table XIX

Equations		Exp.-calc. = v
$6\,S_{Ca} + 6\,S_{Ha}$	$= 1.77326$	+ 7
$1\,S_{Cs} + 3\,S_{Hs} + 6\,S_{Ca} + 5\,S_{Ha}$	$= 2.11442$	- 16
$2\,S_{Cs} + 6\,S_{Hs} + 6\,S_{Ca} + 4\,S_{Ha}$	$= 2.45605$	+ 8
$5\,S_{Cs} + 12\,S_{Hs}$	$= 1.80715$	+ 17
$6\,S_{Cs} + 14\,S_{Hs}$	$= 2.14919$	0
$7\,S_{Cs} + 16\,S_{Hs}$	$= 2.49121$	- 18
$6\,S_{Cs} + 12\,S_{Hs}$	$= 2.05331$	+ 6
		$\Sigma v^2 = 0.1018 \times 10^{-6}$

These equations give least squares values of:

		Difference	
S_{Hs}	0.04797 ± 0.00007	0.00082	1.71 % (8 x probable error)
S_{Ha}	0.04879 ± 0.00010		
S_{Cs}	0.24627 ± 0.00016	0.00047	0.191 % (3 x probable error)
S_{Ca}	0.24674 ± 0.00009		

When the aromatic equations are redrawn after subtracting S_{CH3} the graph of Figure 13 is obtained. The circled points are the values calculated by the least squares method. The probable errors indicated above in the least squares solution are those indicating agreement of the equations used among themselves. Each equation was considered to have equal weight.

On the graph as shown in Fig. 13, the values of S_C and S_H from the pure elements as well as the same quantities calculated from Aron's Tables are also plotted. It will be noticed that the values of both quantities increase progressively from element to saturated to unsaturated. In fact, the three points almost form a straight line. From these values it is possible to calculate the ionization potential by the use of equations XVII and XVIII. To make this calculation the energy is taken as 270 Mev and the ionization potential of copper is taken as 279 following Segrè and Bakker. The calculation of I is relatively insensitive to the energy chosen. The results are given in tabular form below.

Table XX

Condition	I_C	I_H	
element	70.2 e.v.	18.2 e.v.	
aliphatic-sat.	69.3	15.5	
aromatic-unsat.	67.2	13.0	
from CCl_4	57.9		(See Section on Chlorine)

There is no doubt a close correlation between these results and the character of the binding in the compounds considered. Pauling[24], Coulson[25] and others discuss the nature of such bindings in some detail

in the references given. While the relationship is evident it is difficult to be sure at this point exactly what the facts mean and how to interpret them.

The columns in Tables XVI through XIX entitled Exp.-Calc. were computed by subtracting the calculated value of the compound using the least squares solutions above (for S_{Ca}, S_{Cs}, S_{Ha}, S_{Hs}) from the experimental values. Note particularly the homologs pentane, hexane, and heptane. This column shows that there is a small decrease in stopping power as one goes up the homolog chain. This might be considered a fine structure superposed on the general effect. The same effect will be noted also in considering the alcohols. As the effect is very small, it may not be real.

No significant difference has been noticed between liquid and solid samples. Styrene gives a stopping power of 2.362 ± 0.001 and polystyrene 2.357 ± 0.002 approximately. This is a difference of 0.005 or about 0.2 percent. On the other hand styrene has one extra double bond and this may be sufficient to cause the difference. However, in view of the possible lack of homogeneity of the solids and possible structure changes in styrene this difference cannot be held significant.

Another comparison of the same type may be obtained from polyethylene and two aliphatic liquids.

$$\begin{array}{ccccc} C_7H_{16} & - & C_5H_{12} & = & 2CH_2 \\ 2.49121 & & 1.80715 & & 0.68406 \end{array}$$

From the above $CH_2 = 0.34206 \pm 0.0005$

From polyethylene $CH_2 = 0.3432 \pm 0.002$ (est.)

Again, because of larger errors in the solid density determination this cannot be considered significant. The difference in the two results is 0.32 percent.

Since we are also comparing polymers with the unpolymerized material above, it appears that there is little or no effect on polymerization. This is true unless any effect due to polymerization is almost exactly cancelled by an effect in going from solid to liquid or some other change.

It is interesting to note the complete change of character between benzene and cyclohexane, the same ring saturated with 6 more hydrogens. As far as this experiment shows cyclohexane behaves completely like the straight chain saturated aliphatics. This is, of course, to be expected. The saturated methyl side chain in the aromatics also seems to behave like CH_2 in aliphatics. As an example:

$C_6H_5CH_3$	-	C_6H_6	=	CH_2
2.11442		1.77326		0.34116

$CH_2 = 0.34116 \pm 0.0014$

$C_6H_4(CH_3)_2$	-	C_6H_6	=	$2CH_2$
2.35605		1.77326		0.68279

$CH_2 = 0.34138 \pm 0.00039$

From the Figure 13 or the least squares solution of Table XIX, an aromatic CH_2 would give a vlue 0.3443. An aliphatic CH_2 should give a value 0.3422, somewhat lower. The values indicated above seem to show that the CH_3 on the aromatic ring behaves as a saturated aliphatic group as expected.

It appears evident from the foregoing that it should be possible to calculate the stopping power as defined in this paper for any compound of carbon and hydrogen to an accuracy of the order of 0.1 percent or better. For this purpose one need only examine the structures of the compound and add the proper value for each carbon and hydrogen in the structure to give the total stopping power. From this calculated value one can then use known ranges in copper to obtain directly ranges in the compound. Or one can obtain dE/dx for the compound by use of the definition of S and known (dE/dx) values for copper, correcting the S for the compound to put it at the proper energy point as indicated in the section on method.

B. Chlorine

The chlorine compounds considered were chlorinated hydrocarbons. If it is assumed that the results of the carbon-hydrogen determination for S_{Ca}, S_{Cs}, S_{Ha}, and S_{Hs} can be carried over to those also containing chlorine, the stopping power of chlorine may be calculated by subtraction. (See Table XIII.) This operation is carried out in Table XXI.

Table XXI

Compound	Formula	Equation	S_{Cl}	
Carbon Tetrachloride	CCl_4	$\frac{S_{CCl_4} - S_{C_s}}{4} = S_{Cl}$	$= 0.6346 \pm 0.00011$	Saturated
Chloroform	$CHCl_3$	$\frac{S_{CHCl_3} - S_{C_s} - S_{H_s}}{3} = S_{Cl}$	$= 0.6354 \pm 0.00020$	Saturated
1,2 Dichloro-ethane	$C_2Cl_2H_4$	$\frac{S_{C_2Cl_2H_4} - 2S_{C_s} - 4S_{H_s}}{2} = S_{Cl}$	$= 0.6458 \pm 0.001$(est.)	Saturated
Chlorobenzene	C_6H_5Cl	$\frac{S_{C_6H_5Cl} - S_{C_6H_6} + S_{H_a}}{1} = S_{Cl}$	$= 0.6307 \pm 0.0004$	Unsaturated
Ortho Dichlorobenzene	$C_6H_4Cl_2$	$\frac{S_{C_6H_4Cl_2} - S_{C_6H_6} + 2S_{H_a}}{2} = S_{Cl}$	$= 0.6332 \pm 0.0005$	Unsaturated
Trichloroethylene	C_2Cl_3H	$\frac{S_{C_2Cl_3H} - 2S_{C_a} - S_{H_a}}{3} = S_{Cl}$	$= 0.6338 \pm 0.00021$	Unsaturated
Tetrachloro-ethylene	C_2Cl_4	$\frac{S_{C_2Cl_4} - 2S_{C_a}}{4} = S_{Cl}$	$= 0.6334 \pm 0.0001$	Unsaturated

The errors here assigned are compounded from those due to the internal consistance of runs on the C-H-Cl compounds and to the values obtained for S_C and S_H by least squares. The samples chlorobenzene, ortho-dichlorobenzene, trichloroethylene, tetrachloroethylene and 1,2 dichloro-ethane (often called ethylenedichloride) were single samples. Several different samples of chloroform and carbon tetrachloride were used and perhaps more reliance may be placed on these results. The results for 1,2 dichloroethane may be in error as it was run only once by the current method and was of technical grade purity. The value for chlorobenzene appears low compared to the rest. This may possibly be due to impurities, as only one sample was run. It might also represent a real effect. The saturated linkages in chloroform, carbon tetrachloride, and 1,2-dichloro-ethane indicate a stopping power for chlorine somewhat higher than the unsaturated linkages of the other compounds considered. If dichloro-ethane is not considered, one obtained values as follows:

Saturated Hydrocarbon	Scl	0.6350 ± 0.0003
Unsaturated Hydrocarbon Including Chlorobenzene	Scl	0.6328 ± 0.0009
Unsaturated Hydrocarbon (No Chlorobenzene)	Scl	0.63346 ± 0.00028
All Compounds (except Dichloro-ethane)	Scl	0.6335 ± 0.0035

It will be noticed that the difference between the saturated and the unsaturated values is small and of the order of 0.3 percent, and

at least twice the probable error. This change in stopping power need not be attributed solely to the chlorine atoms. If it is assumed that the unsaturated chlorine value obtained from the compounds represents a more reasonable value, then one may attribute this change in stopping power of the compound to a further reduced mean ionization potential for carbon, corresponding to an increased stopping power. In these more complex molecules the effects are not simple and the attempt here can be looked upon as no more than a start at an explanation.

If the above value of 0.6335 is assumed to hold for all chlorine atoms then the value obtained from carbontetrachloride for carbon is 0.2509 ± 0.0008. For chloroform using the aromatic hydrogen value it is 0.2512 and using the aliphatic hydrogen value, it is 0.252 ± 0.001.

Using 0.2509 as the value for S_C the mean ionization potential for carbon is C-cl compounds is 57.9 e.v.

Such an interpretation might seem to indicate that the valence electrons of carbon spend a much smaller amount of time in the vicinity of the carbon nucleus in carbon-chlorine compounds, due to the tendency for chlorine to form negative ions, and draw the electrons away from the carbon.

Using Equation XVII and XVIII the mean ionization potential for chlorine (S_{Cl} = 0.6335) is 153.7 ev. if I_{copper} = 279 e.v.

C. Oxygen

The compounds of oxygen considered were water, five alcohols, two ethers, and one ketone. If it be assumed that the values already used for carbon and hydrogen in saturated compounds hold in this case, we may use these to subtract from the observed stopping power to obtain the stopping power of oxygen. (See Table XIV.) The value used for the hydrogen in the OH radical is that for the aliphatic hydrogen. The errors assigned in Table XXII are those due to compounding the error quoted from internal consistency of each compound run as indicated above with the errors of S_C and S_H calculated by the least square method. (See Table XXII.)

The values calculated in Table XXII for oxygen agree quite well. The type of binding of the oxygen in all cases but that of acetone is such that two other atoms are bound or linked together by oxygen. The results of the alcohols and ether all seem comparable and give for the stopping power of oxygen:

$$S_O = 0.3187 \pm 0.0024$$

The error here calculated is based upon agreement of the results for S_O obtained from the various compounds. The value of S_O is that calculated using the unweighed results given in Table XXII. The agreement with molecular oxygen is excellent. It is worth noting that the stopping power of oxygen increases slightly as one passes from methyl to ethyl

Table XXII

Oxygen-Carbon-Hydrogen

Formula	Stopping Power	Subtract		S_o	(Mean-S_o) Residual
O (Molecular)	0.3188 ± 0.0003(est.)			0.3188 ± 0.0003	+ 0.00010
H_2O	0.41411 ± 0.000083	H2	(0.09594)	0.31817 ± 0.00013	- 0.00051
$(C_2H_5)_2O$	1.78457 ± 0.00048	$(C_2H_5)_2$	(1.51275)	0.31979 ± 0.00063	+ 0.00109
CH_3OH	0.75449 ± 0.0005	CH_4	(0.43815)	0.31716 ± 0.001(est.)	- 0.00152
C_2H_5OH	1.09875 ± 0.00014	C_2H_6	(0.78036)	0.31839 ± 0.00035	- 0.00029
C_3H_7OH	1.44149 ± 0.0005(est.)	C_3H_8	(1.12257)	0.31892 ± 0.001(est.)	+ 0.00022
C_4H_9OH	1.78460 ± 0.001(est.)	C_4H_{10}	(1.46478)	0.31982 ± 0.001(est.)	+ 0.00112
$C_3H_5(OH)_3$	2.07896 ± 0.00066	C_3H_8	(1.12257)	0.31880 ± 0.0003	+ 0.00010
C_3H_6O	1.34920 ± 0.00034	C_3H_6	(1.02663)	0.32257 ± 0.00045	

to n-propyl to normal butyl alcohol. Although the effect is small and only about as large as the probable error, it may be real and might possibly indicate a gradual increase in stopping power of the compound as a whole with an increasing length of carbon chain. Referring back to the carbon-hydrogen compounds again, it may be noted that a homolog effect occurs there between pentane, hexane, and heptane. It is much smaller in the latter case. The direction in the hydrocarbon case is such as to reduce slightly the compound stopping power with increasing chain length. If this effect can be believed, it would seem to indicate that the oxygen affects several adjacent atoms as predicted by Coulson[25]. These effects are of the order of the probable errors and therefore remain doubtful.

The value for S_o from acetone is 1.2 percent higher than the mean value and the difference is about six times the probable error. The type of binding in this case is a double bonded oxygen and is rather different than the binding in the other compounds considered. The results might therefore be expected to be somewhat different.

From Equation XVII and XVIII, the value obtained for the ionization potential for oxygen is:

Alcohols, etc.	$I_o(-O-) = 88.5$ ev.
Acetone	$I_o(O=) = 79.8$ ev.
Molecular Oxygen	$= 88.3$

D. Nitrogen

The compounds of nitrogen considered were nitrobenzene, analine, and pyridine. Each exhibits a somewhat different type of nitrogen binding. The stopping powers for the nitrogen compounds are given in Table XV.

If we assume the values from other elements of similar composition as follows:

$$S_{Ha} = 0.04879 \pm 0.0001$$

$$S_{Ca} = 0.24674 \pm 0.0009$$

$$S_{o} = 0.32257 \pm 0.00045 \quad \text{(taking value from acetone)}$$

The values of S_N calculated are as follows:

Compound	S_N	I Value
Nitrobenzene	0.2782 ± 0.0024	89.4 e.v.
Analine	0.2788 ± 0.002	
Pyridine	0.2870 ± 0.0021	68.8
Elementary	0.2837 ± 0.0002	76.3

From the above it appears that the results of the nitrobenzene and the analine are quite comparable. However, the result of pyridine is high far beyond the experimental error. It is not too surprising that this is true as the binding of nitrogen in pyridine must differ markedly from that in the other two compounds. Note also in this case that the liquid gas value falls in between the other two values. The agreement between nitrobenzene and analine may only be fortuitous.

VI. CONCLUSIONS

This experiment has shown that the relative stopping power of various compounds for a high energy proton beam (270 Mev mean energy in target) is an additive function of the elements making up the compound to within about 1 percent.

However, it has shown quite definitely that there exist small, but measurable, deviations from the strict additivity of the stopping powers of elements to form the stopping powers of compounds. In general, these deviations are in such a direction as to raise the relative molal stopping power as defined in this experiment. This corresponds to a lowering of the mean ionization potential. As expected, the percent deviation from additivity decrease with increasing atomic number.

The experiment has measured to a high degree of accuracy the stopping power of four elements, hydrogen, carbon, nitrogen, and oxygen. The stopping power of a fifth element, chlorine, may be approximated closely from its compounds. (These data were given in the abstract of this paper as Table I.)

Table I

Element	S	I
Hydrogen (Molecular)	0.0472 ± 0.0002(est.)	18.2 ev.
Carbon (Graphite)	0.2455 ± 0.0005(est.)	70.2 ev.
Nitrogen (Molecular)	0.2837 ± 0.0001(est.)	76.3 ev.
Oxygen (Molecular)	0.3188 ± 0.0003(est.)	88.3 ev.
Chlorine (from cpds.)	0.6335 ± 0.0035	153.7 ev.

A table of stopping powers may be set up from which, by proper selection and addition, the stopping powers of most compounds of these elements can be computed to an accuracy probably better than 0.1 percent. (These data were given in the abstract of this paper as Table II.)

Table II

Element	Position in Compound	S	I
Hydrogen	Saturated	0.04797 ± 0.00007	15.5 ev.
	Unsaturated	0.04879 ± 0.00010	13.0
Carbon	Saturated	0.24627 ± 0.00016	69.3
	Unsaturated	0.24674 ± 0.00009	67.2
	Highly chlorinated	0.2509 ± 0.0008	57.9
Nitrogen	Amines, nitrates, etc.	0.2785 ± 0.0025	89.4
	In ring	0.2870 ± 0.0020	68.8
Oxygen	-O-	0.3187 ± 0.0024	88.5
	=O	0.3226 ± 0.0010	79.8
Chlorine	All	0.6335 ± 0.0035	153.7

As an example, let us use the values worked out in this paper to calculate the stopping power of β-β' dichlorodiethyl ether ($C_4H_8OCl_2$)

4 Saturated Carbons	4x0.24627	0.98508
8 Saturated Hydrogens	8x0.04797	0.38376
1 (-O-) Oxygen	1x0.31870	0.31870
2 Chlorines	2x0.63346	1.26692
		Σ = 2.95446 ± 0.001
Experimental value		= 2.95528 ± 0.0005
		Δ = 0.00083 or 1/3700

From this value, the definition of S, and the range or dE/dx for copper one can calculate ranges or dE/dx values for the compound.

It is possible that the experiment has suggested a new means of attack on chemical binding problems. Further study and refinement may bring to light methods of applying these and other stopping power results to supplement thermochemical data. Attempts are being made by the author and others to formulate a satisfactory interpretation of the effects observed.

VII. ACKNOWLEDGMENTS

I would like to express my sincere thanks to Dr. Emelio Segrè and to Dr. Owen Chamberlain for helpful advice during the course of this work. I would also like to thank Dr. H. Bethe for helpful discussions on the theory of stopping power as applied to this experiment. I am very grateful to James Easley and Robert Main for assistance in constructing the absorber changing system. Charles Godfrey was entirely responsible for the redesign of the Peterson liquid hydrogen target and was of invaluable assistance during the liquified gas runs. Thanks are due to James Vale, Lloyd Houser, and the crews of the 184-inch synchrocyclotron for their efficient operation of the machine during the runs. Frank Vaughn, Bob Main, James Easley, Noel Spiess and Jack Garrison were very helpful during the course of the various cyclotron runs involved.

VIII. REFERENCES

1. N. Bohr, Phil Mag., 24, 10 (1913), 30, 581, (1915).
2. H. Bethe, Annalen der Physik, 5, 325, (1930).
3. H. Bethe, Handbuck der Physik, 24, 273, (1933).
4. M. S. Livingston and H. Bethe, Rev. Mod. Phys. 9, 263, (1937).
5. P. M. S. Blackett, Proc. Roy. Soc. 135, 132, (1932).
6. W. E. Duncanson, Proc. Camb. Phil. Soc. 30, 102, (1934).
7. R. R. Wilson, Phys. Rev., 60, 749, (1941).
8. J. H. Smith, Phys. Rev., 71, 32, (1947).
9. C. J. Bakker and E. Segrè, Phys. Rev., 81, 489, (1941).
10. R. Mather and E. Segrè, Phys. Rev., 84, 191, (1951).
11. J. A. Wheeler and R. Ladenburg, Phys. Rev., 60, 754, (1941).
12. F. Bloch, Zeits. f. Physik., 81, 363, (1933).
13. N. Bloembergen and P. J. van Heerden, P.R., 83, 561, (1951).
14. A. E. Taylor, Reports on Progress in Physics, Vol. XV, 49, (1952).
15. W. A. Aron, B. G. Hoffman, F. C. Williams, University of California Radiation Laboratory Report 121 (1949).
16. Jahnke-Emde, Tables of Functions (1933)-B. G. Teuber (Leipzig).
17. National Research Council, International Critical Tables, Vol. III, McGraw-Hill, 1928.
18. C. A. Coulson, Nature, 159, 265, (1947).
19. S. Mrozowski, Phys. Rev., 85, 609, (1952).
20. V. Peterson, University of California Radiation Laboratory Report No. 713, May, (1950).
21. R. B. Scott, F. B. Brickwedde, J.R.N.B.S., 19, 237, (1937), R.P. 1023.
22. H. J. Woolley, R. B. Scott, F. B. Brickwedde, J.R.N.B.S., 41, 33, (1948), R.P. 1932.

23. O. Chamberlain, E. Segrè, C. Wiegand, Phys. Rev., 83, 923, (1951).

24. L. Pauling "The Nature of the Chemical Bond", Cornell University Press, 1945.

25. C. A. Coulson, Chem. Soc. London Quarterly Reviews 1, 144, (1947).

IX. ILLUSTRATIONS

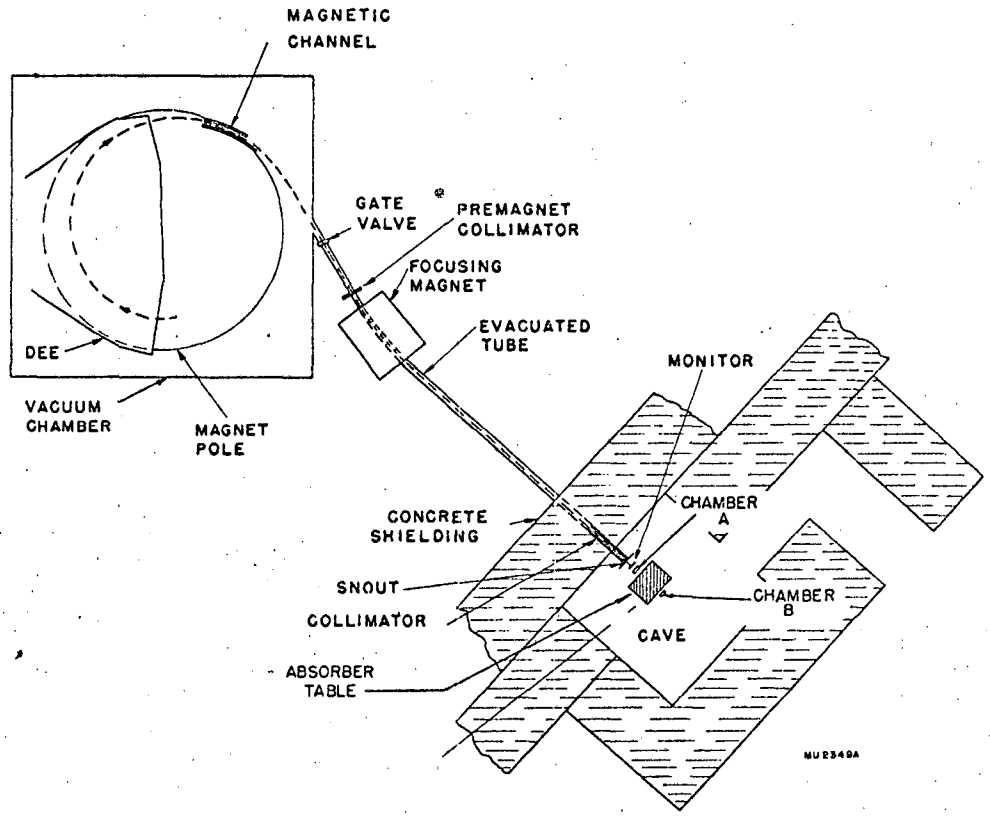
MAGNETIC
CHANNEL
GATE
VALVE
PREMAGNET
COLLIMATOR
FOCUSING
MAGNET
EVACUATED
TUBE
DEE
VACUUM
CHAMBER
MAGNET
POLE
MONITOR
CHAMBER
A
CONCRETE
SHIELDING
SNOUT
COLLIMATOR
CHAMBER
B
CAVE
ABSORBER
TABLE
MU2349A

Fig. 1

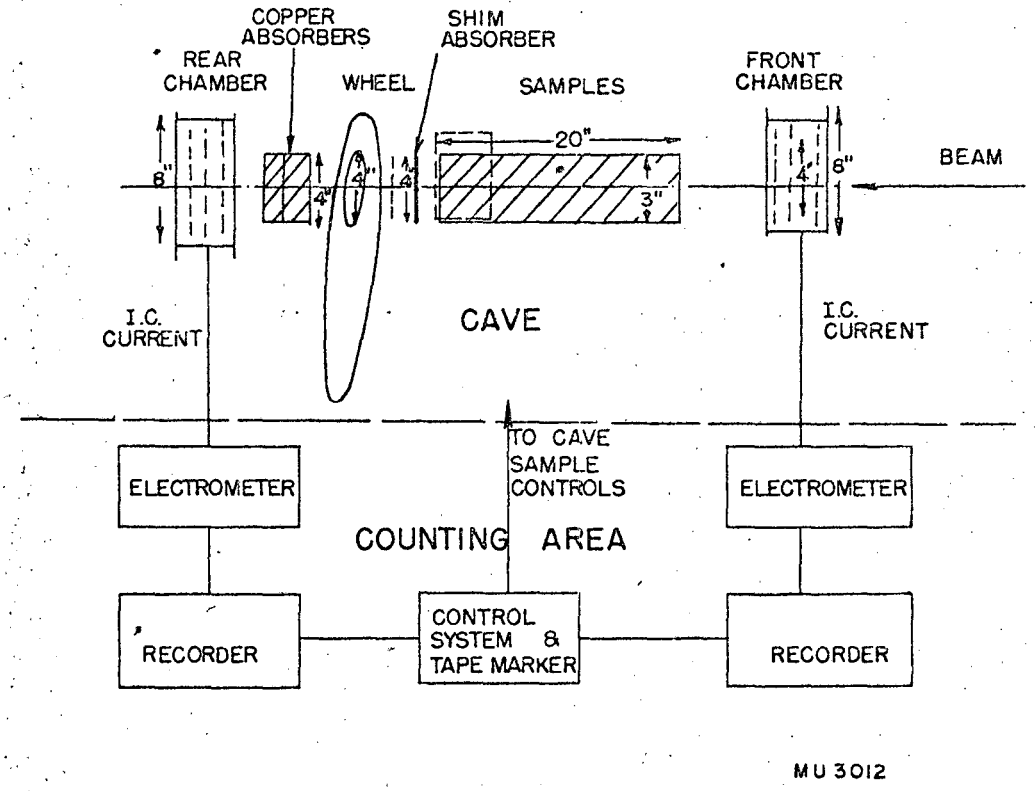
COPPER ABSORBERS
SHIM ABSORBER
REAR CHAMBER
WHEEL
SAMPLES
FRONT CHAMBER
20"
8"
4"
4"
4"
3"
6"
BEAM
I.C. CURRENT
CAVE
I.C. CURRENT
TO CAVE SAMPLE CONTROLS
ELECTROMETER
ELECTROMETER
COUNTING AREA
RECORDER
CONTROL SYSTEM & TAPE MARKER
RECORDER
MU 3012

Fig. 2

Fig. 3

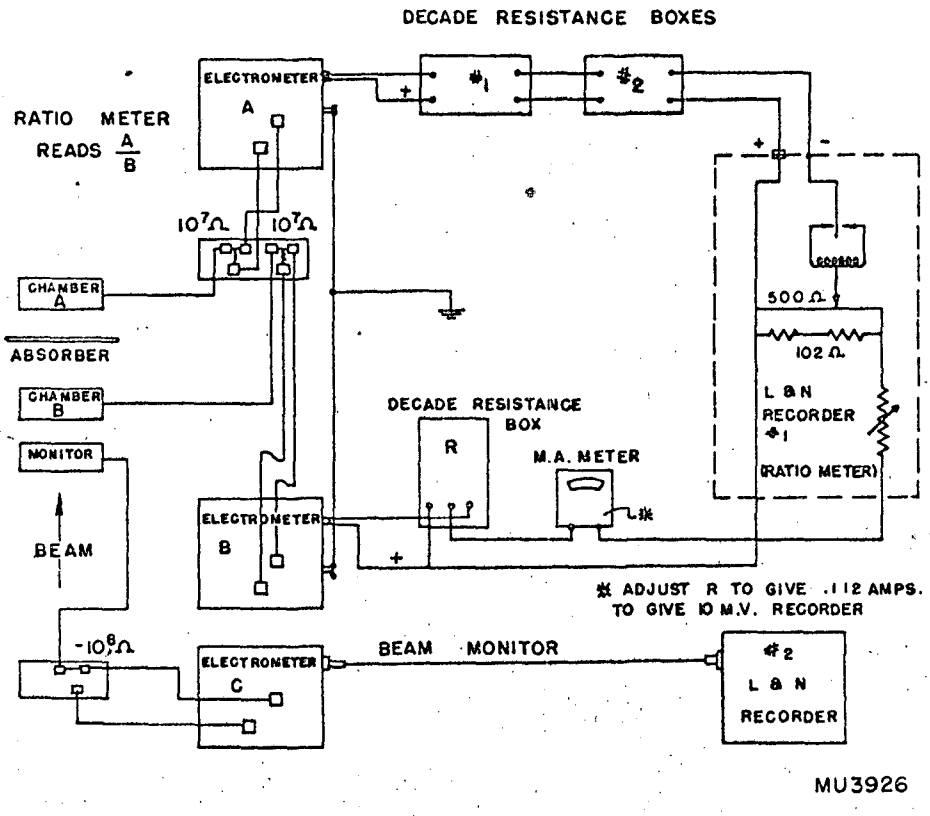
DECADE RESISTANCE BOXES
ELECTROMETER
A
RATIO METER
READS A/B
#1
#2
10⁷Ω
10⁷Ω
CHAMBER
A
ABSORBER
CHAMBER
B
MONITOR
BEAM
500Ω
102Ω
L & N
RECORDER
#1
(RATIO METER)
DECADE RESISTANCE
BOX
R
M.A. METER
ELECTROMETER
B
* ADJUST R TO GIVE .112 AMPS.
TO GIVE 10 M.V. RECORDER
-10⁸Ω
ELECTROMETER
C
BEAM MONITOR
#2
L & N
RECORDER
MU3926

Fig. 4

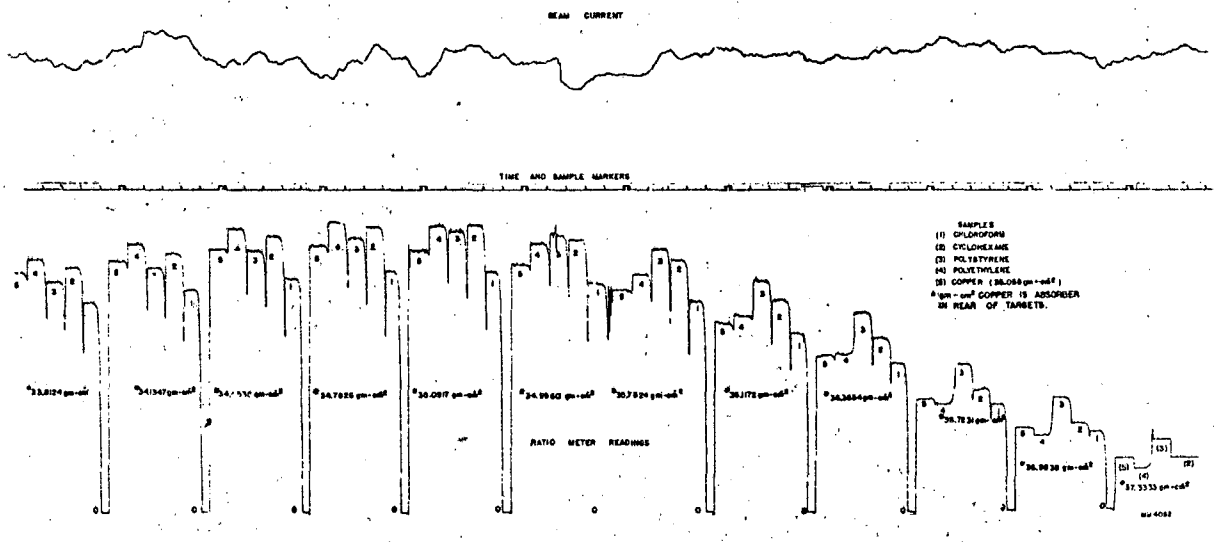
BEAM CURRENT
TIME AND SAMPLE MARKERS
SAMPLES
(1) CHLOROFORM
(2) CYCLOHEXANE
(3) POLYSTYRENE
(4) POLYETHYLENE
(5) COPPER (8808.0 gm-cm²)
* gm - cm² COPPER IS ABSORBER IN REAR OF TARGETS.
RATIO METER READINGS

Fig. 5

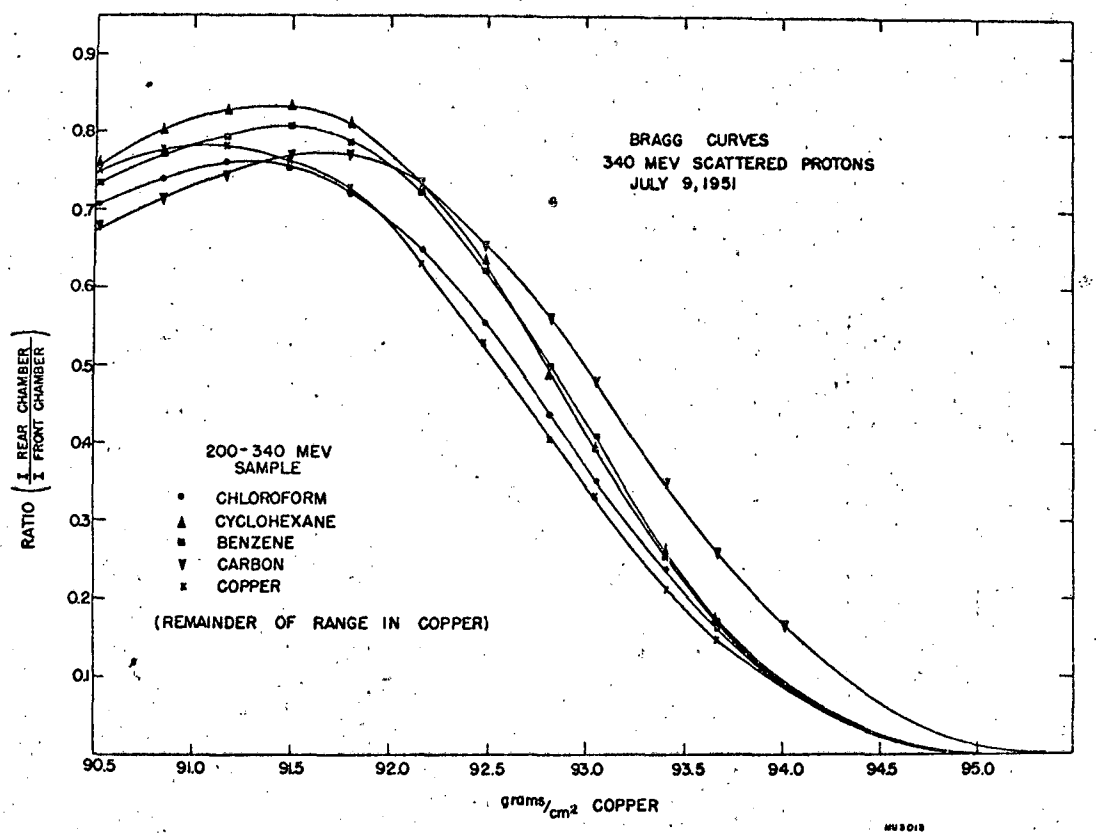
BRAGG CURVES
340 MEV SCATTERED PROTONS
JULY 9, 1951
200-340 MEV
SAMPLE
CHLOROFORM
CYCLOHEXANE
BENZENE
CARBON
COPPER
(REMAINDER OF RANGE IN COPPER)
RATIO (I REAR CHAMBER / I FRONT CHAMBER)
0.9
0.8
0.7
0.6
0.5
0.4
0.3
0.2
0.1
90.5
91.0
91.5
92.0
92.5
93.0
93.5
94.0
94.5
95.0
grams/cm² COPPER

Fig. 6

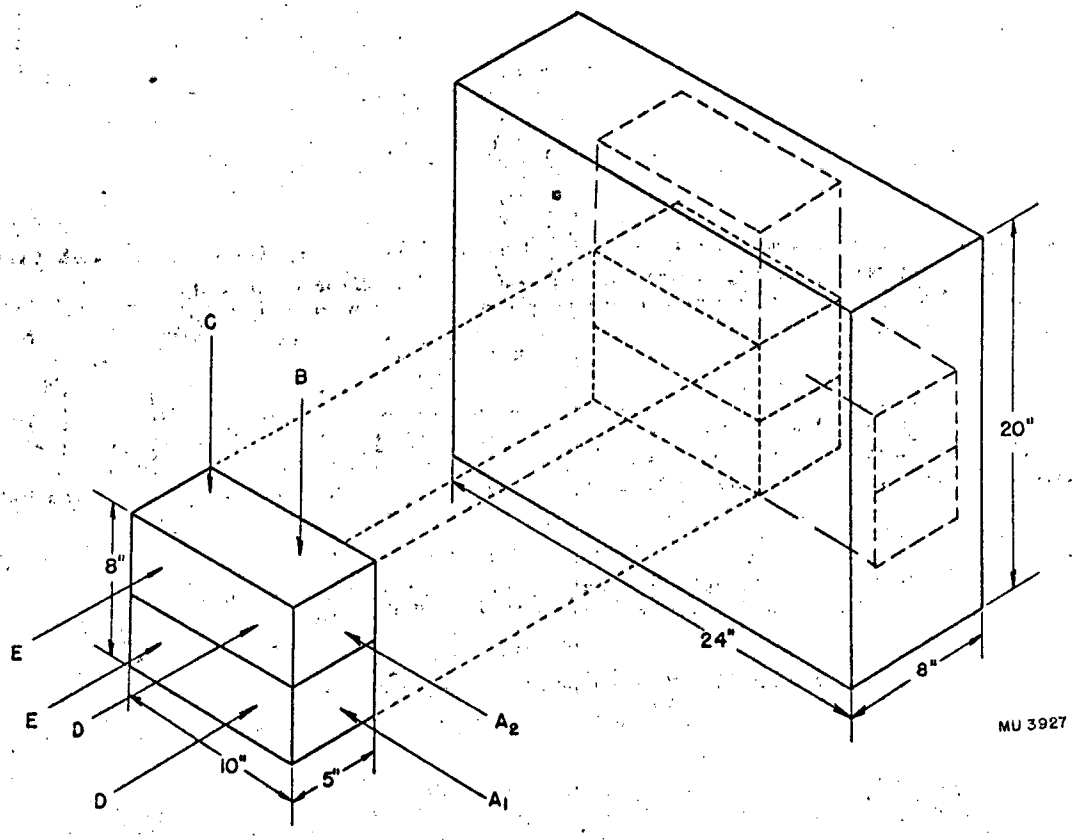

Fig. 7

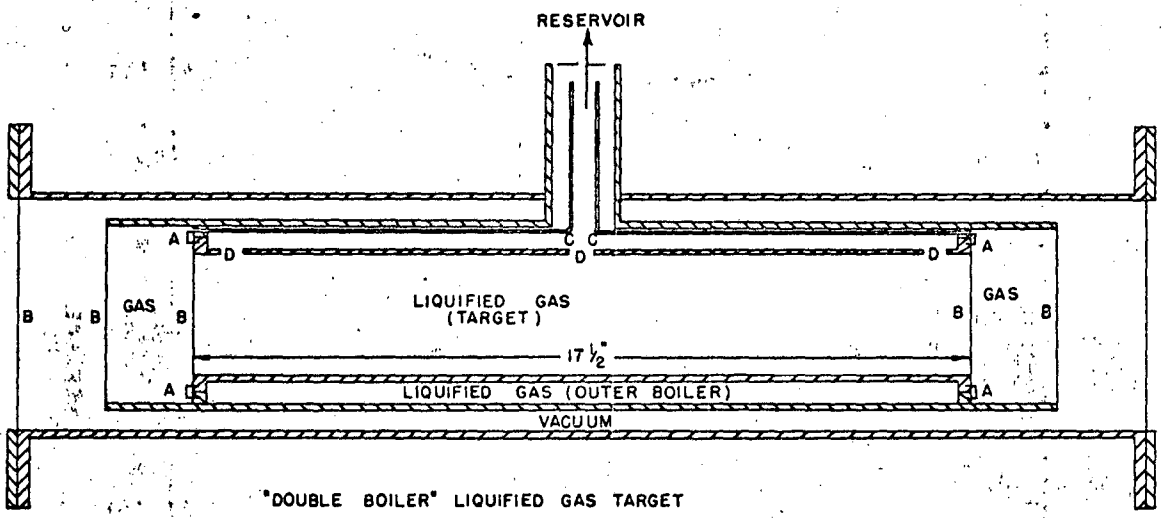

"DOUBLE BOILER" LIQUIFIED GAS TARGET

A = FLEXIBLE METAL U SHAPED RING SEALING OFF GAS CHAMBERS, (ALLOWS FOR UNEVEN EXPANSION OF CONCENTRIC TUBES)

B = THIN METALLIC WINDOWS

C = TUBES VENTING END GAS CHAMBERS TO AIR OR GAS

D = VENTS IN INNER TUBE

MU4037

Fig. 3

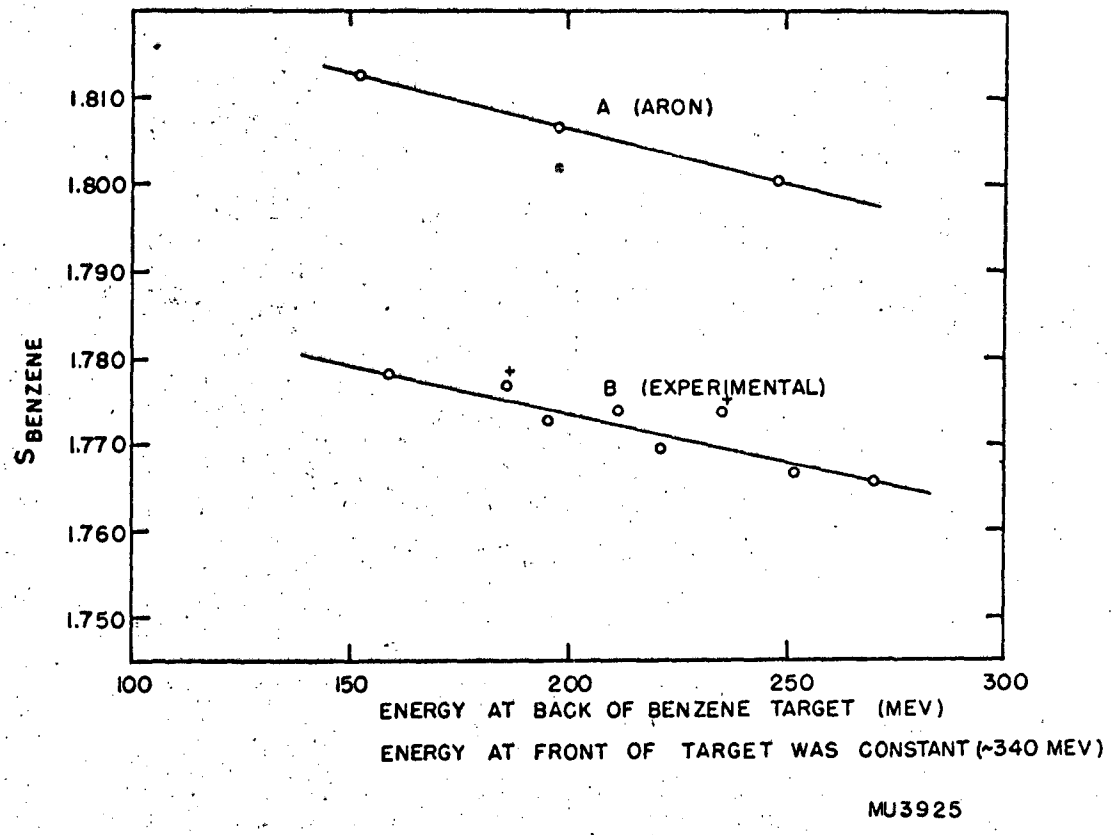
1.810
1.800
1.790
1.780
1.770
1.760
1.750
S BENZENE
A (ARON)
B (EXPERIMENTAL)
100
150
200
250
300
ENERGY AT BACK OF BENZENE TARGET (MEV)
ENERGY AT FRONT OF TARGET WAS CONSTANT (~340 MEV)
MU3925

Fig. 9

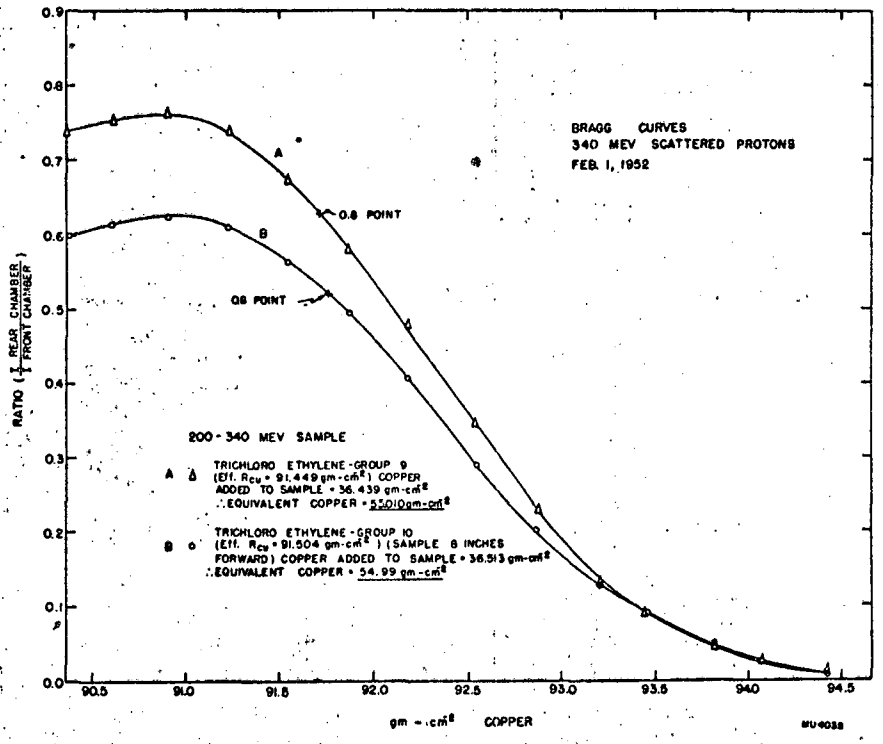
BRAGG CURVES
340 MEV SCATTERED PROTONS
FEB. 1, 1952
A
0.8 POINT
B
0.8 POINT
200 - 340 MEV SAMPLE
A Δ TRICHLORO ETHYLENE - GROUP 9
(Eff. R_{Cu} = 91.449 gm-cm²) COPPER
ADDED TO SAMPLE = 36.439 gm-cm²
∴EQUIVALENT COPPER = 55.010 gm-cm²
B ○ TRICHLORO ETHYLENE - GROUP 10
(Eff. R_{Cu} = 91.504 gm-cm²) (SAMPLE 8 INCHES
FORWARD) COPPER ADDED TO SAMPLE = 36.513 gm-cm²
∴EQUIVALENT COPPER = 54.99 gm-cm²
RATIO (REAR CHAMBER / FRONT CHAMBER)
0.0
0.1
0.2
0.3
0.4
0.5
0.6
0.7
0.8
0.9
90.5
91.0
91.5
92.0
92.5
93.0
93.5
94.0
94.5
gm - cm² COPPER
MU-4038

Fig. 10

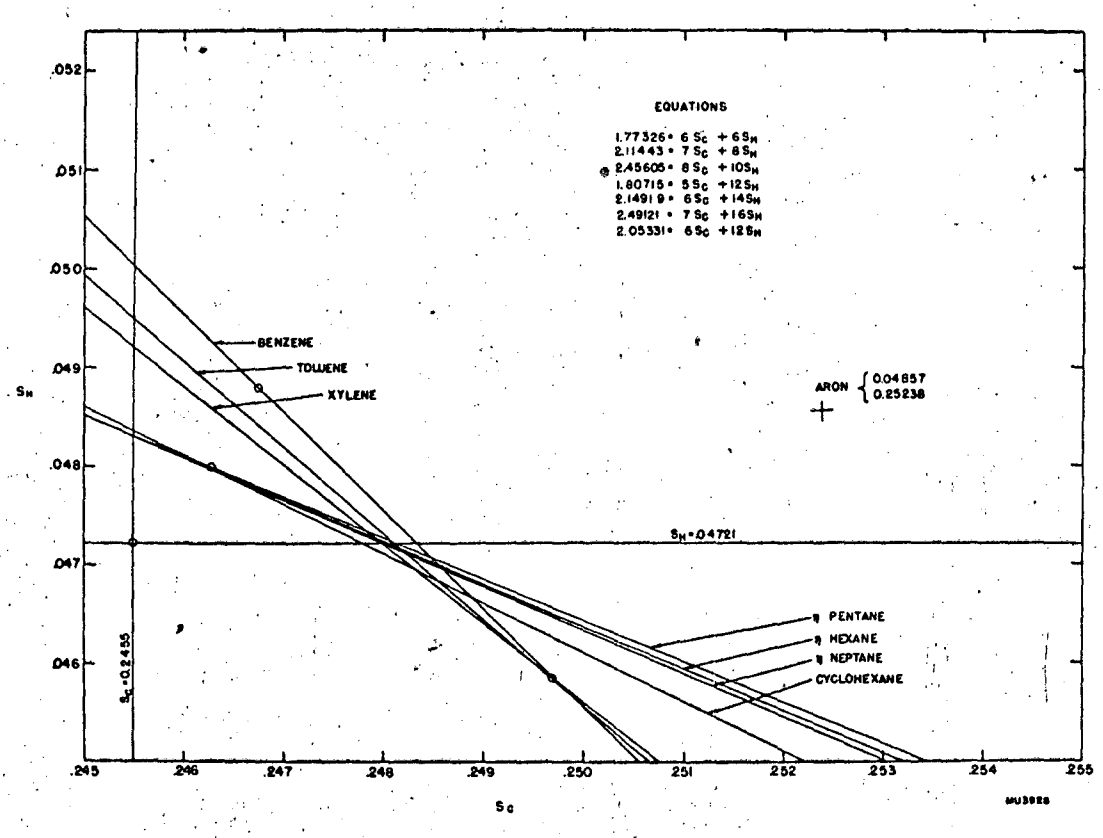
EQUATIONS
1.77326 + 6 Sc + 6 SH
2.11443 + 7 Sc + 8 SH
2.45605 + 8 Sc + 10 SH
1.80715 + 5 Sc + 12 SH
2.14919 + 6 Sc + 14 SH
2.49121 + 7 Sc + 16 SH
2.05331 + 6 Sc + 12 SH
BENZENE
TOLUENE
XYLENE
ARON 0.04857
0.25238
SH = 0.4721
Sc = 0.2455
n PENTANE
n HEXANE
n HEPTANE
CYCLOHEXANE
SH
Sc
.052
.051
.050
.049
.048
.047
.046
.245
.246
.247
.248
.249
.250
.251
.252
.253
.254
.255

Fig. 11

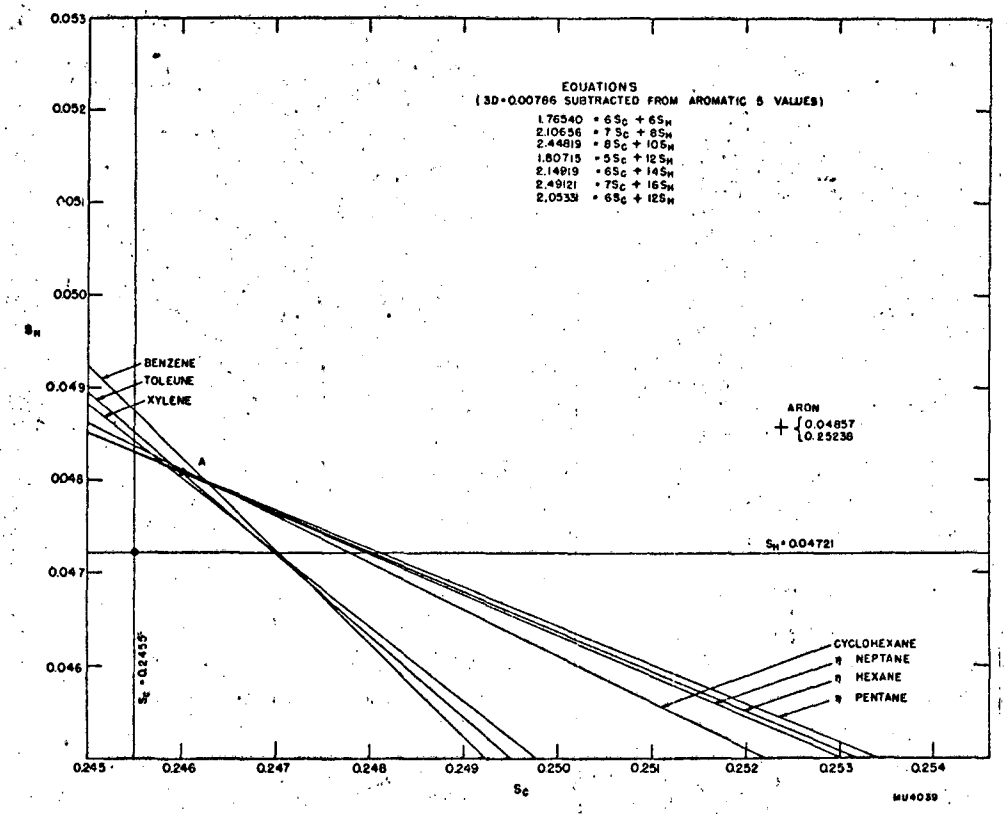
EQUATIONS
(3D=0.00766 SUBTRACTED FROM AROMATIC δ VALUES)
1.76540 = 6Sc + 6SH
2.10656 = 7Sc + 8SH
2.44819 = 8Sc + 10SH
1.80715 = 5Sc + 12SH
2.14919 = 6Sc + 14SH
2.49121 = 7Sc + 16SH
2.05331 = 6Sc + 12SH
ARON
+ {0.04857 0.25238
BENZENE
TOLUENE
XYLENE
A
SH = 0.04721
Sc = 0.2455
CYCLOHEXANE
n NEPTANE
n HEXANE
n PENTANE
δH
Sc
0.053
0.052
0.051
0.050
0.049
0.048
0.047
0.046
0.245
0.246
0.247
0.248
0.249
0.250
0.251
0.252
0.253
0.254
MU4039

Fig. 12

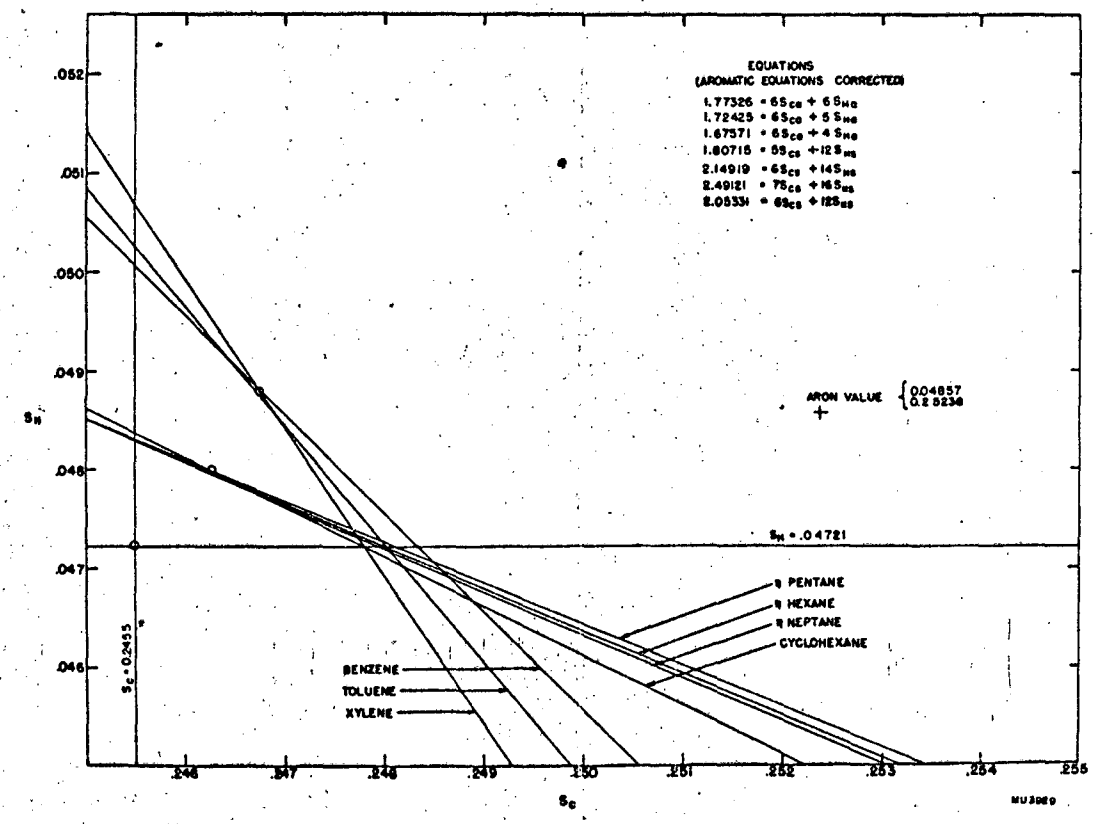
EQUATIONS
(AROMATIC EQUATIONS CORRECTED)
1.77326 = 6S_CO + 6S_HO
1.72425 = 6S_CO + 5S_HO
1.67571 = 6S_CO + 4S_HO
1.80715 = 5S_CO + 12S_HO
2.14919 = 6S_CO + 14S_HO
2.49121 = 7S_CO + 16S_HO
2.08334 = 6S_CO + 12S_HO
ARON VALUE
.004857
0.2 .0238
S_H = .04721
S_C = .02455
n PENTANE
n HEXANE
n HEPTANE
CYCLOHEXANE
BENZENE
TOLUENE
XYLENE
.052
.051
.050
.049
.048
.047
.046
S_H
.246
.247
.248
.249
.250
.251
.252
.253
.254
.255
S_C
MU3989

Fig. 13